2020

Introducing Functionality to Poly(arylene ether)s via Modification of Diphenyl sulfone – type Monomers

Zahida Humayun
Wright State University

INTRODUCING FUNCTIONALITY TO

POLY(ARYLENE ETHER)S, VIA MODIFICATION OF

DIPHENYL SULFONE – TYPE MONOMERS

A thesis submitted in partial fulfilment of the

requirements for the degree of

Master of Science

by

ZAHIDA HUMAYUN

B.S., Quaid-i-Azam University, Pakistan, 1998

2020

Wright State University

WRIGHT STATE UNIVERSITY

GRADUATE SCHOOL

April 30, 2020

I HEREBY RECOMMEND THAT THE THESIS PREPARED UNDER MY

SUPERVISION BY Zahida Humayun ENTITLED Introducing Functionality to Poly (arylene ether)s, via Modification of Diphenyl sulfone – type Monomers BE ACCEPTED IN PARTIAL FULFILMENT OF THE REQUIREMENTS FOR THE DEGREE OF Master of Science.

_____

Eric Fossum, Ph.D.

Thesis Director

_____

David A. Grossie, Ph.D.

Chair, Department of Chemistry

Committee on Final Examination:

_____

Eric Fossum, Ph.D.

_____

Daniel Ketcha, Ph.D.

_____

Ioana Pavel, Ph.D.

_____

Barry Milligan, Ph.D.

Interim Dean of the Graduate School

ABSTRACT

Humayun, Zahida. M.S. Department of Chemistry, Wright State University, 2020.
Introducing Functionality to Poly(arylene ether)s via Modification of Diphenyl sulfone-type Monomers.

The synthesis of poly(arylene ether)s, with a pendent aryl iodide, was achieved via nucleophilic aromatic substitution (NAS) polycondensation of DI-DFDPS monomer. The platform diiodo-difluorodiphenyl sulfone monomer, DFDPS-DI (**3**), was prepared in one-step, via EAS chemistry. Structural characterization was provided by NMR spectroscopy, GC/MS, and elemental analysis. As "pre" approach didn't work here, so "post" approach was used to synthesize *N*-heterocycle functionalized copolymers. The DI-copolymers were subjected to copper-catalyzed C-N coupling reaction with carbazole, phenoxazine, and indole and the syntheses of chromophore based copolymer were successfully carried out. A series of PAEs containing carbazole, phenoxazine, and indole substituents were synthesized and characterized. The copolymers were characterized by a combination of NMR spectroscopy, UV/Vis spectroscopy. DI-copolymers displayed had sufficient molecular weight (M_n) and thermal stability with 5% weight loss temperature (T_g) above 388 ^{0}C and glass transition temperature, T_g, value above 193 ^{0}C. Optical analyses provided that all modified copolymer materials emitted in the light blue region.

TABLE OF CONTENTS

1. INTRODUCTION

LIST OF FIGURES

LIST OF TABLE

LIST OF SCHEMES

ACKNOWLEDGMENTS

I would like to thank my thesis advisor, Dr. Eric Fossum for all his guidance, patience, and for sharing his knowledge and experience throughout the program. I have learned a lot in my time here and for that I will always be grateful. I would like to thank my committee members, Dr. Daniel Ketcha and Dr. Ioana Pavel, for their guidance and knowledge. I would also like to thank Dr. Fossum's Research Group, in particular Hannah, Brandon, Garrett, and Sophia, for all their help. Thank you to the Wright State University Department of Chemistry. I would like to thank the faculty and staff members, in particular Dr. Ioana Pavel for allowing us to use her instrumentation for this project.

I would like to thank my family, especially my son Aaliyan, my husband, Zeeshan and sister Esha, for all of their love and support throughout the program.

1. INTRODUCTION

1.1 Organic Light Emitting Diodes

Organic Light Emitting Diode (OLED) devices have been in continuous development since the early 1960s. OLEDs have attracted considerable attention as a source of lighting and flat screen displays during the past decades. The fist diode device was reported at Eastman Kodak by Ching W. Tang and Steven Van Slyke in 1987.[1] In 1990, J.H. Burroughes reported a high efficiency green light-emitting polymer-based device. In 1996, Pioneer produced the world's first commercial polymer OLED. Since 2000 many companies such as Motorola, LG, Sony, etc. have developed various display technologies. Sony developed the world's largest full color OLED in 2001 and, in 2008, introduced an OLED television.[2]

OLED utilize organic materials to emit light. The OLED technology has attracted significant attention due to its ease of fabrication and the potential to be produced via low cost pathways, especially when compared to more traditional LED materials. For example, the use of inkjet printing and spin coating processes are possible with all organic systems. Due to their potential for superior performance, cost savings, and processing advantages, OLEDs are currently considered as the next-generation lighting and display technology.

1.2 Structure of OLED

An OLED (see **Figure 1**) is essentially a solid-state semiconductor device that is 100 to 500 nanometers thick. The organic layers have a thickness of ~100-200 nm while the overall devices are only a few millimeters in thickness. OLEDs are a class of materials with self-emitting properties that require no backlighting to operate.[3] Light is usually produced through conversion of an electrical current to emission, commonly

1

referred to as electroluminescence (EL), a characteristic that many conjugated, organic molecules share.

OLEDs typically consist of a series of organic thin films sandwiched between two thin conductive electrodes. There are many choices for each layer, depending upon the application. The substrate is usually made up of glass but may be made of polyethylene plastic for a flexible display, which act as a platform/foundation for the rest of the device. The anode is made up of indium-tin-oxide (ITO). The surface of ITO is rough and mechanical flexibility of ITO is very poor due to its ceramic structure.[4] Due to indium scarcity, the ITO cost of production is high. Among the available conducting polymers, poly(3,4-ethylenedioxythiophene: polystyrene sulfonate, (PEDOT:PSS) has attracted considerable attention for the excellent electrical and optical properties.[4] It smooths the anode surface and prevents the short-circuiting of device due to sharp spikes on the ITO surface. The PSS doped PEDOT exhibits good optical properties but less conductivity due to presence of insulating PSS in the PEDOT matrix. Since PEDOT:PSS has low conductivity, it is only used as a buffer layer in the electronic devices.[4]

Poly(3,4-ethylenedioxythiophene)
polystyrene sulfonate
[PEDOT:PSS]
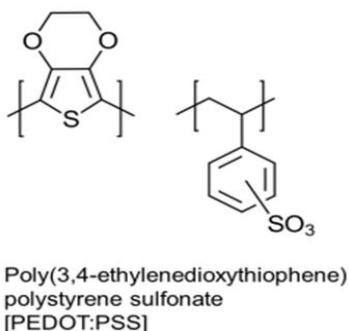
The hole transport layer (HTL) is deposited on the top of anode. For HTL materials, properties such as efficient hole injection and enough hole mobility are important as the total current of OLED is governed by hole current. This layer receives holes from the anode and transports them to the emissive layer, EML. The most common hole transport materials are N,N'-diphenyl-N,N'-bis(3-methylphenyl)(1,1'-biphenyl)-4,4'-diamine (TPD) and N,N'-bis(1-naphthyl)-N,N'-diphenyl-1,1'-biphenyl-4,4'-diamine (NPB).The emissive layer is the heart of the device, where the light is produced. The color of the light depends on the structure of the organic molecules in the emissive layer. Manufacturers place several layers of organic films on the same OLED to make multi-

color displays. The electron transport layer (ETL), made of polyaniline is next to the cathode and supports the transport of electrons across it so they can reach the emissive layer. 2,2',2''-(1,3,5-benzenetriyl)-tris(1-phenyl-1-*H*-benzimidazole) (TmPyPB) can be used as electron-transporting (ETL) material.[5] Some other electron-transport/Hole blocking layers are BCP (2,9-Dimethyl-4,7-diphenyl-1,10-phenanthroline), BmPyPB (1,3-bis[3,5-di(pyridin-3-yl)phenyl]benzene), and TmPyPB (1,3,5-tri(p-pyrid-3-yl-phenyl)benzene). The cathode is usually made up of an aluminum or magnesium alloy because aluminum is readily available with a high purity, and low cost. It is negatively charged, which injects electrons into the organic electron transporting layer. Multiple organic layers can be put in place to increase device efficiency and lifetime.[3] It is also important to note that the anode and cathode layers must be a very uniform thickness to minimize the chance of short-circuiting the device. Due to the large chemical variability of organic layers, thin, flexible properties, and expected lifetimes higher than that of LEDs, drive the development of these devices immensely.
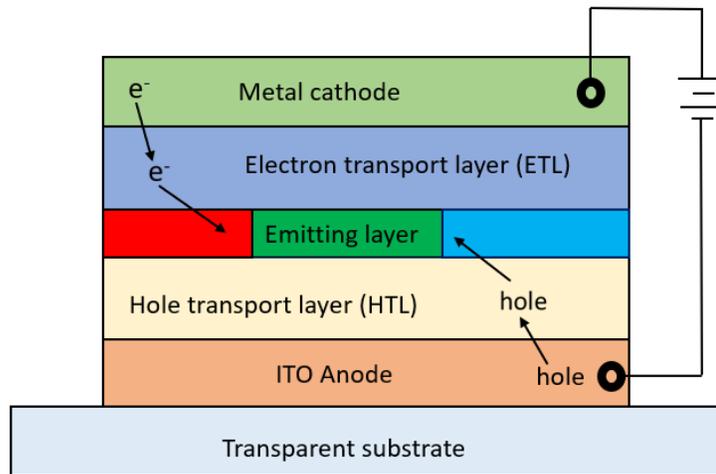
Figure 1. Light Emission for an OLED.

1.3 Working principle of OLEDs

During the operation, a forward bias voltage is applied from the anode to the

3

cathode. This allows electrons to be injected from the cathode into the LUMO of the ETL and holes to be injected from the anode into the HOMO of the HTL. The recombination of electrons and holes occurs in the emissive layer (EML). Sometimes the EML may be the ETL, HTL, or a separate layer between these one or the other layer, but not both. The emitted light may pass through the substrate unobstructed, if substrate being used is a glass or plastic substrate.[6]

1.4 Bandgap (E_g)

The energy difference between the highest occupied molecular orbital (HOMO) and the lowest unoccupied molecular orbital (LUMO) of a molecule is known as the bandgap. The bandgap is directly related to the wavelength of emission. As shown in **Figure 2**, a red emission requires a bandgap of approximately 1.9 eV, while green and blue need 2.34 and 2.70 eV, respectively. OLED devices require a combination of red-green-blue (RGB) emitters to give a full color display. The different bandgaps also lead to long term stability and efficiency issues. The large bandgap characteristic of blue emitters leads to problems with molecular stability, as well as poor compatibility with most host materials.[7] A large bandgap makes compounds more susceptible to degredation via oxidation pathways.
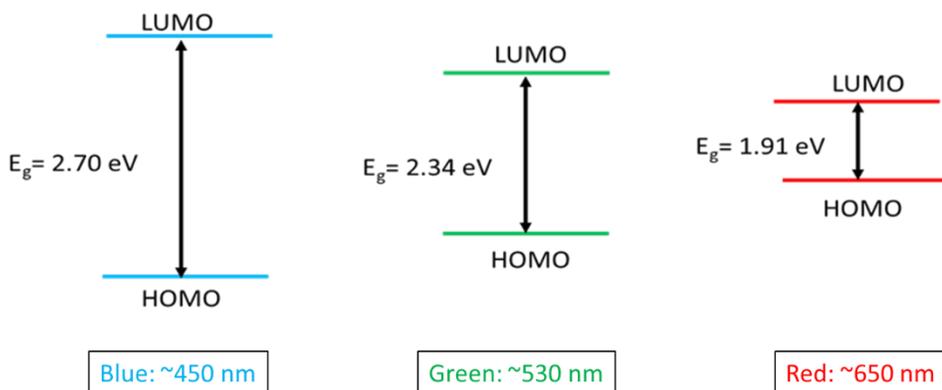
Figure 2. Band gap for HOMO-LUMO energy level.

1.5 Three generations of OLED (Emission Mechanisms):

In general, electroluminescence materials form two different types of excitons, singlet excitons have a spin S = 0 and triple excitons with S = 1. The relative probability for the formation of singlet and triplet excitons is 25% to 75% respectively according to the spin statistics from quantum mechanics.[7] For efficient OLEDs, it
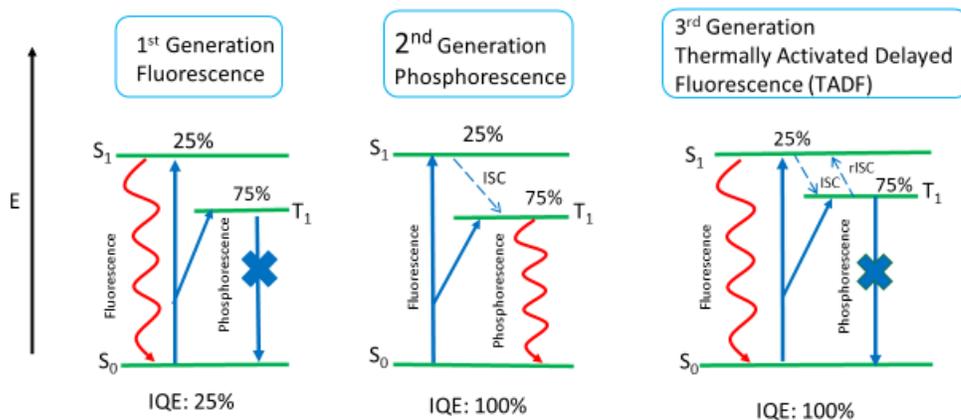
Figure 3. Emission Mechanisms: fluorescence, phosphorescence and TADF.

is important to harvest both singlet and triplet excitons for the generation of photons.[7] Three main emissive mechanisms, fluorescence, phosphorescence and TADF are available to harvest excitons.

1.5.1 1st Generation OLED: Fluorescence

The first way to achieve electroluminescence is through traditional fluorescence. The energy difference between the singlet state S_1 and the triplet state T_1 is relatively large and the triplet excitons are unable to be harvested due to the T_1 to S_1 transition being spin-forbidden. The energy differences between these two states is called the singlet-triplet energy barrier or $\triangle E_{st.}$
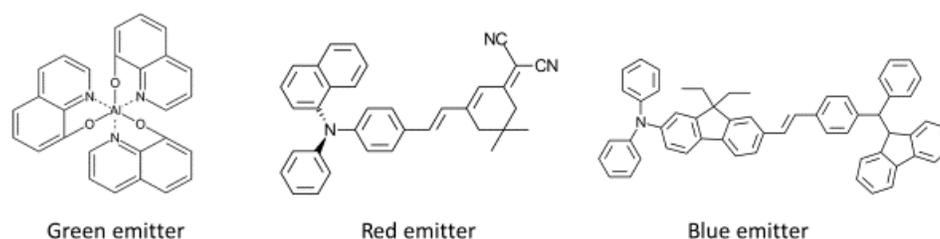
Figure 4. From left to right, green, red, and blue fluorescent emitting molecules for OLED devices.

The fluorescent small molecules show the immediate emission of absorbed radiations. Some examples of small fluorescent molecules used in OLED devices are given in **Figure 4.** Tris(8-hydroxyquinolinato) aluminum (Alq$_3$) (left) is a green fluorescent OLED emitter. Alq$_3$ is a complex in which aluminum is bonded to three 8-hydroxyquinoline ligands. A blue emitting molecule (right **Figure 4**), exhibits a maximum absorption wavelength of 386 nm and a fluorescence wavelength of 465 nm, at a concentration of 10^{-5} M, in dichloromethane.[9] The naphthylamine derivative (center, **Figure 4**) is an example of a red fluorescent emitter. This molecule showed an efficient emission peak at 676 nm as a thin film.[10]

1.5.2 2nd Generation OLED: Phosphorescence

Phosphorescent molecules show delayed emission of absorbed radiation.

These molecules have a large $\triangle E_{st}$. OLEDs containing Ir(III), Pt(III), or Os (II) based phosphors can harvest both singlet (25%) and triplet (75%) exitons through heavy atom enhanced intersystem crossing (ISC).[11] The intersystem crossing (ISC) is very strong, leading to a transition of any singlet into triplet excitons. So, the phosphorescent molecules can harvest all the triplet excitons as photons via the triplet state T$_1$, resulting in highly efficient OLEDs. For example, blue phosphorescent molecules using iridium-based complexes show emission of peak at ~468 nm.[12]

6
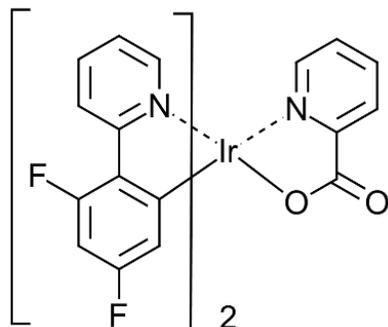
Figure 5. An iridium-based blue phosphorescent molecule.

1.5.3 3rd Generation OLED: Thermally Activated Delayed Fluorescence

Third generation TADF emitters have small singlet-triplet energy gaps between the Singlet (S_1) and triplet state (T_1), allowing ISC and rISC.[13] This small energy difference allows the triplet excitons to shift to the singlet state and emit photons via the fluorescence pathway, resulting in ~ 100% internal quantum efficiency. Transitions between T_1 and S_0 are still forbidden, however, by mean of rISC, they can go from T_1 back to S_1 and all excitons are harvested via the singlet state S_1.

In 2012, Adachi et al.[14] reported on utilizing rISC for fluoresence molecules or the transition of electrons from T_1 to S_1. For this to occur efficiently, the emitting molecules must have small $\triangle E_{st}$ between the T_1 and S_1 energy levels.

1.6 TADF Emitters

All TADF emitters consist of donor and acceptor moieties.[7] Donors are usually electron rich molecules/groups and associated with the HOMO. On the other hand, the acceptors are electron poor/deficient molecules/groups and are associated with the LUMO.[7] These groups are linked by π-bonds, thus the name donor-π-acceptor systems.

7

TADF donor moieties are electron-rich functional groups. There are various common donor units like carbazole, acridine, phenoxazine, phenothiazine and their derivatives that can be used for a TADF system.
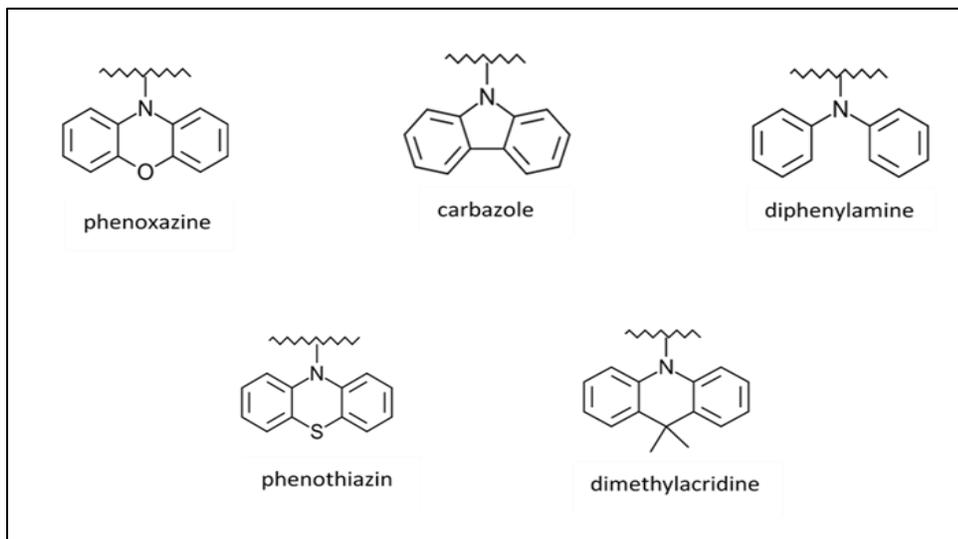
Figure 6. Structures of various TADF donor units.[15]

There are various types of acceptor systems **(Figure 7)** including diphenyl sulfone derivatives, benzonitrile derivatives, and *N*-heterocyclic derivatives that can be used for a TADF system.
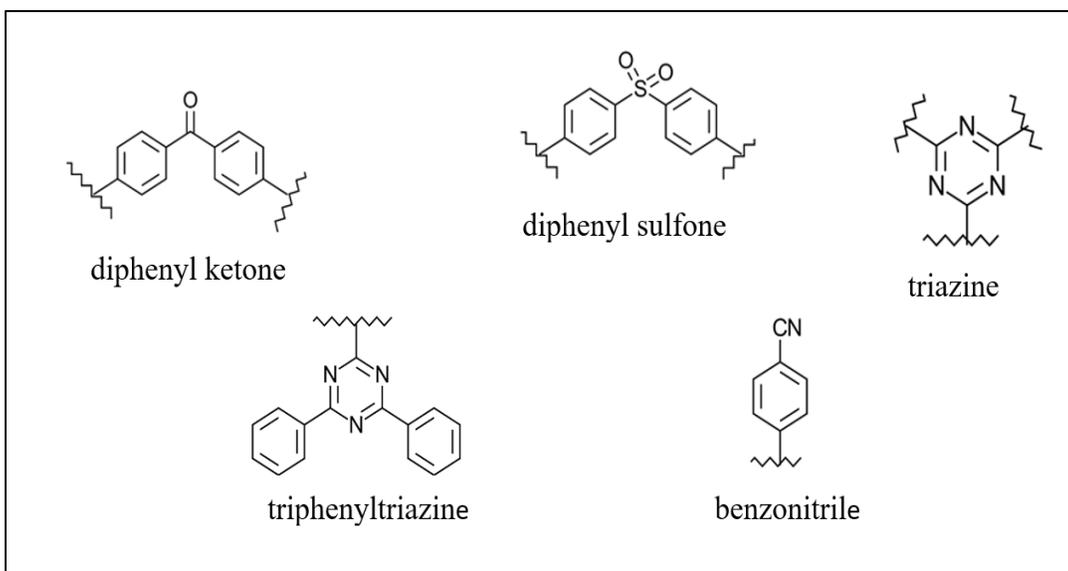
Figure 7. Structures of various TADF acceptor units.[15]

Various combinations of donors and acceptors have been used to make molecules emitting different wavelengths. In a TADF molecule, the donor and acceptor may be tuned to get emission of specific bandgap. An example of a molecule (6-(9,9-dimethylacridin-10(9H)-yl)-2-phenyl-1H-benzo[de]isoquinoline-1,3(2H)-dione) that produces emission in the red region is given in **Figure 8** (left).[16] The observed wavelength of emission was 597 nm. The BIQ (6-acridine-benzo iso quinoline) moiety which is the electron deficient part, has two carbonyl units conjugated to a naphthalene backbone structure to allow for electron accepting character and low emission energy for red emission. A strong dimethylacridine donor was combined with a BIQ acceptor for small singlet-triplet energy splitting (ΔE_{st}) and a red-shift of emission wavelength.[16]
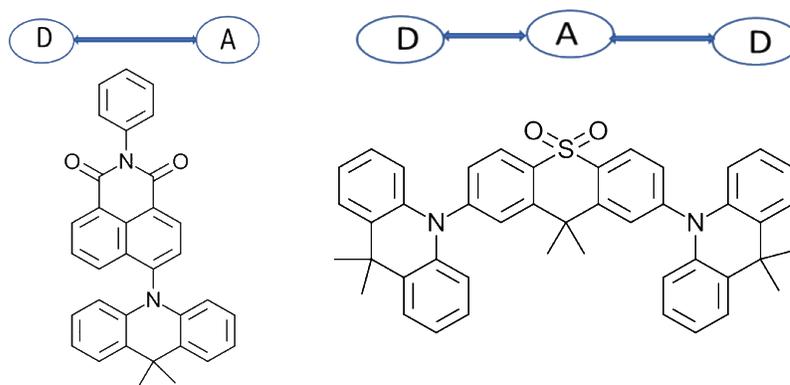
 Figure 8. Red emitter, small TADF molecule (Left), Deep blue TADF emitter, DMTDAc (Right).

In the TADF molecule at right (**Figure 8**),[17] 9,9-dimethyl-9H-thioxanthene 10,10-dioxide was used as acceptor unit and the acridine was chosen as a donor unit. This blue emitter molecule (404 nm) showed high efficiency due to its very slight overlap of HOMO and LUMO, and $\Delta E_{st} = 0$ eV.

To achieve a TADF molecule, a donor-acceptor system is needed. If the HOMO and LUMO levels have a good separation, a small ΔE_{st} will be obtained. The small ΔE_{st} can be manipulated by alternating the structures of the donor and acceptor. With the appropriate choice of donor and acceptor units connected through the π-

bonds (D-π-A), the color can be tuned to desired wavelength.[5]
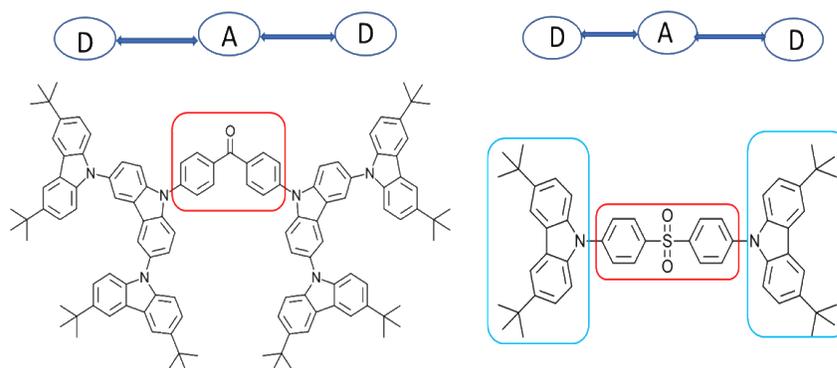
Figure 9. TADF molecules wih wavelength in green (left) and blue (right) emission region.

An example of a molecule that emits in the green region can be seen in **Figure 9. (Left).**[18] The acceptor part is the benzophenone core and is associated with LUMO level whereas the carbazole derivative is donor part of molecule and is associated with HOMO level. The molecule showed an emission peak at 522 nm from a phosphorescence emission spectrum as a film.[18] The diphenyl sulfone system can be used as an electron acceptor and carbazole and its derivatives can be used as electorn donor in thermally activated delayed fluorescence. An example of a molecule with the emission in blue region has a diphenyl sulfone as an acceptor unit, associated with LUMO level and carbazole as a donor unit, associated with HOMO level. The molecule displayed the emission at 404 nm in toluene and 423 nm when doped with a bis[2-(diphenylphosphino)phenyl] ether oxide (DPEPO) in a film.[13] In 2012, the compounds shown in the **Figure 10** were synthesized by the Adachi group, and was the big break-through for designing blue TADF emitters.[18] These three molecules synthesized used a sulfone system with various carbazole derivatives. All three compounds emitted in the deep blue region of 402-419 nm, with $\triangle E_{st}$ values ranging from 0.54 eV to 0.32 eV.
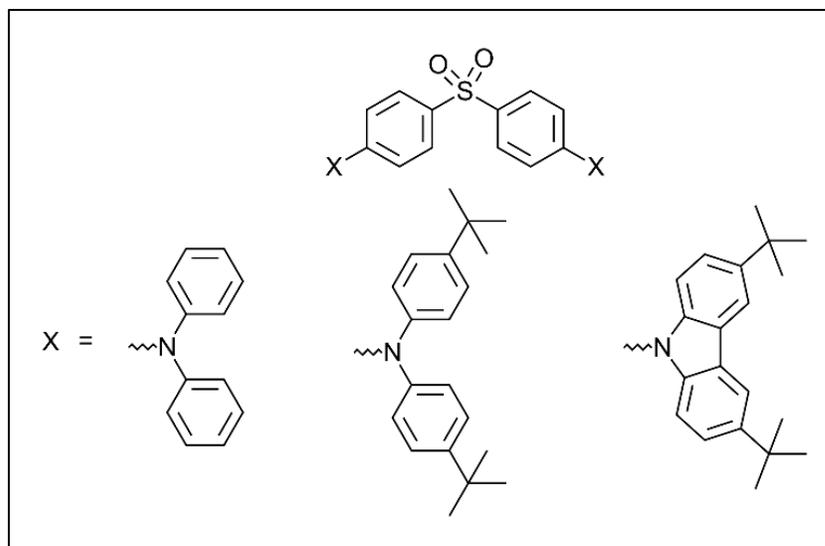
Figure 10. Blue emitting TADF small molecules.[11]

One characteristic which is important in TADF molecule is the twist angle of the donor unit with respect to the acceptor unit. A larger twist angle will break the conjugation from the donor and the acceptor which will result into more separated HOMO and LUMO. The more separated HOMO and LUMO will allow for a small ΔE_{st}, allowing for ISC and rISC to occur allowing for a TADF molecule to exist.[7]

The molecule, bis(3-9,9-dimethyl-9,10-dihydroacridine)phenyl)sulfone (mSOAD), [20] given below, is an acridine/sulfone derivatives. The 9,9-dimethyl-9,10-dihydroacridine (DMAC) was linked to the DPS core via meta-linkage, which leads to highly twisted zig-zag configuration, resulting in a small singlet-triplet energy gap, $\Delta E_{st} = 0.02$ eV, via the spatial distribution of HOMO and LUMO of TADF molecule.[19] When excited at 310 nm, it showed emission centered at 474 nm in solution.
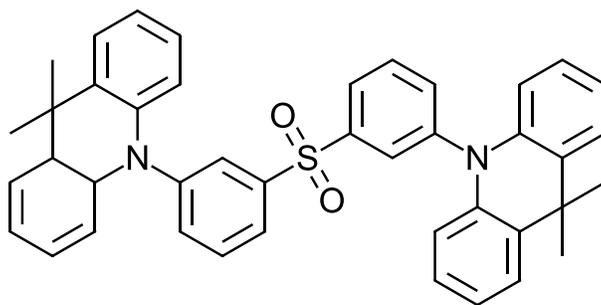
Small OLED, TADF emitters have several advantages, but the methods of fabrication hinder their applications. Because TADF emitters readily crystallize, they are not easily processed by solution based methods. In small molecule OLEDs, the deposition onto the substrate is typically done by a vacuum deposition method.[6] This process gives a uniform thickness of layer to create an OLED device, but at a high cost and of limited use for large-area devices.

1.7 Polymer OLED

Originally, the most basic polymer OLED (PLED), consisted of a single organic layer. The first OLED device was synthesized by J. H. Burroughes et al., and involved a single layer of poly(p-phenylene vinylene). Multilayer OLEDs can be fabricated with two or more layers in order to improve device efficiency. The electroluminescent polymers used in PLED display include: conducting polymers polyaniline (PANI:PSS) and polyethylenedioxythiophene (PDOT:PSS) and emissive polymers, poly(p-phenylenevinylene) (PPV) and polyfluorene (PF).

Conducting Polymers:
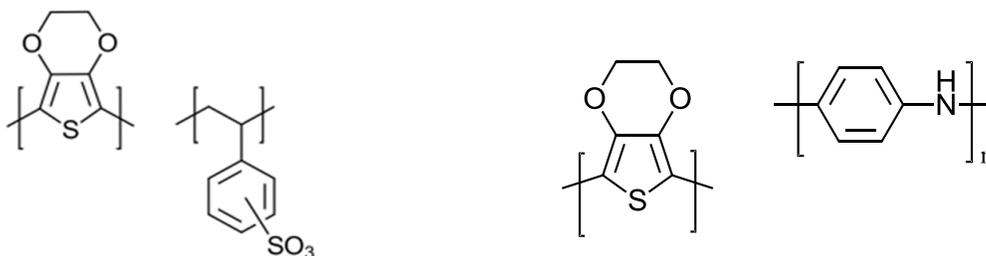
Figure 11. Polyethylenedioxythiophene (PEDOT:PSS)

Polyaniline (PANI:PSS)

Emissive Polymers:
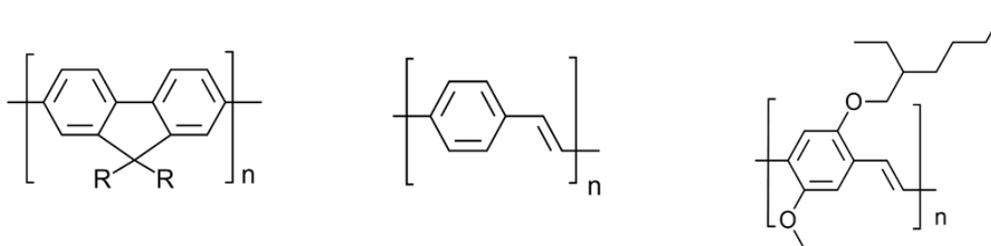
Figure 12. (from left to right) Polyfluorene,blue emitter, PPV (poly(p-phenylenevinylene), green emitter, and poly[(2-(2-ethylhexyioxy)-5-methoxy-p-phenylene)vinylene], (DPVBI), red emitter.

Polymer OLEDs use special types of chromophore containing polymers. Both conjugated and non-conjugated polymers of various structures have been prepared and use each of the three types of emission pathways. Because of 100% IQE of TADF emission, TADF has become an appealing/emerging option for PLED researchers. Polymeric TADF emitting material are attractive candidates because of their low-cost solution processes, such as spin coating and inkjet printing.[20] These methods are useful in making large-area films and are inexpensive too.

TADF polymers must follow the same basic rule as TADF small molecules. In a TADF polymer, the donor and acceptor are connected to allow for a small $\triangle E_{st}$ which allow for efficient reverse intersystem crossing (rISC), and therefore gives 100% electron harvesting. However, it can be difficult to get efficient and strong

luminescence together.

The TADF molecules can be incorporated into polymer using four general strategies (See **Figure 13**): 1) alternating donor and acceptor units in the backbone, 2) alternating TADF molecules with backbone units, 3) donor groups based backbone of polymer with acceptor units grafted as side-chain, and 4) backbone of the polymer with
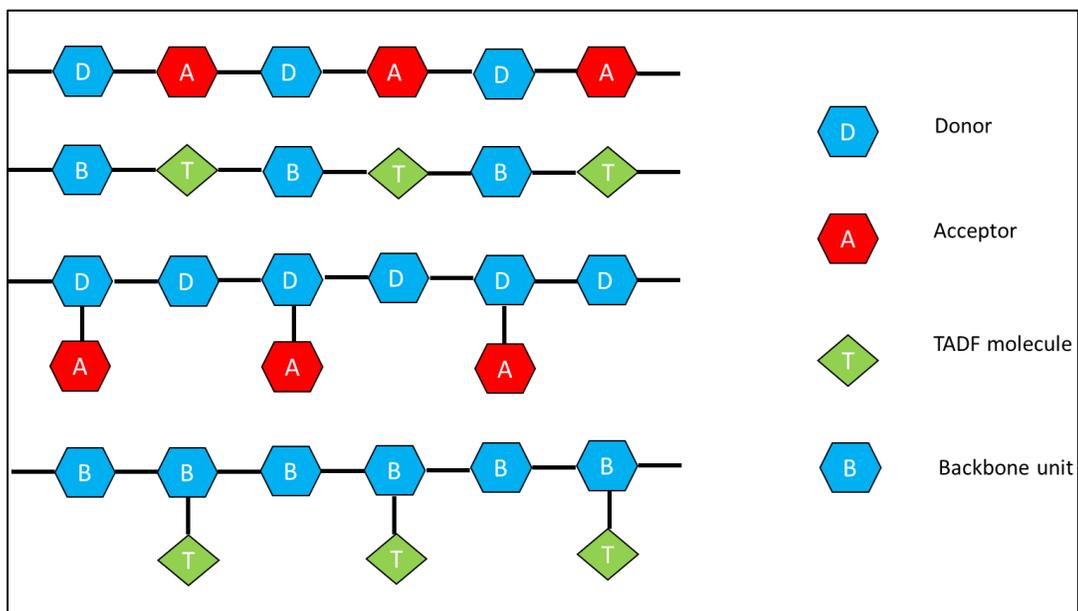
Figure 13. [15] TADF-based polymers Designs.

TADF units as a pendant molecule. The above figure was modeled after the one utilized by Xie and Li.[15] The reverse of method 3, in which an acceptor molecule is incorporated into the backbone unit as a pendant molecule will be used in the current project.

In a TADF molecules, the donor and acceptor may be tuned to get emission of specific bandgap. The acceptor molecule in the TADF polymer shown in **Figure 14** is 9,9-dimethyl-9H-thioxanthene-S,S-dioxide and the donor is acridine. This molecule has $\triangle E_{st}$ of 0.03 eV, because the overlap of HOMO and LUMO is very less, which makes it an efficient emitter. This polymer, in an oxygen-free toluene solution, has a maximum emission wavelengths of 441 nm and 444 nm and 445 nm.[21]
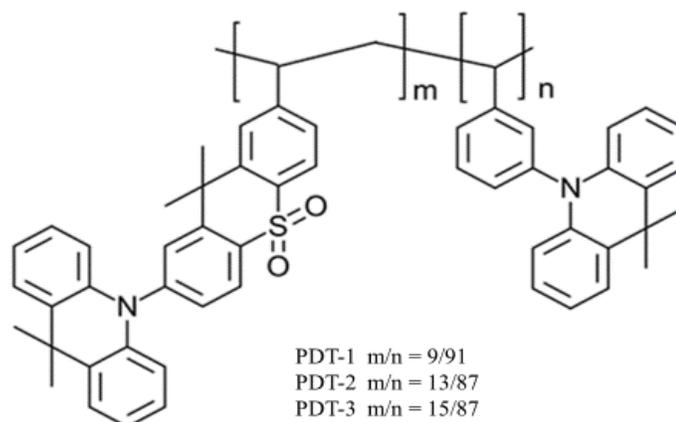
Figure 14. TADF Blue emitter molecule as a pendant in copolymer.

Another method of achieving a TADF-based polymer is to incorporate TADF units as pendant groups. For example, Bryce and coworkers,[22] prepared a copolymer of styrene and phenothiazine chromophore system with iterations using 0.80:0.20, 0.70:0.30 and 0.50:0.50 molar ratios of them, as shown in **Figure 15.** The TADF group
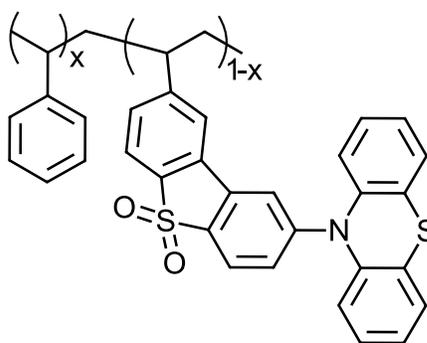
Figure 15. TADF molecule as a pendant in copolymer.[22]

itself was composed of a sulfone electron acceptor group attached to a phenothiazine electron donor, providing a green emission between 535 and 556 nm. The pendent benzene as a spacing agent, was proven to enhance the performance of the TADF properties, by reducing the intramolecular and intermolecular triplet-triplet annihilation of adjacent TADF units. Another observed trend was that as the styrene comonomer unit was increased in molar ratio, the T_1 state increased in energy while

the $\triangle E_{st}$ values were kept small.

1.8 Poly(arylene ether)s, PAE

Poly(arylene ether)s, PAEs, are a type of thermoplastic with good mechanical and chemical properties. A general structure of PAE can be represented as in the **figure 16.** Their structures consist of aromatic rings connected by ether bonds. They have excellent
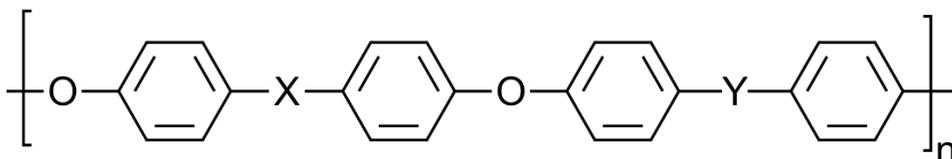
Figure 16. General representation of PAEs backbone structure.

thermal stability and mechanical properties due to the presence of rigid aromatic groups in their backbone. Thermoplastics are easily processed, and they have ability to be molded and remolded without losing material integrity in their physical properties. PAEs have excellent resistance to hydrolysis and oxidation. These thermoplastics possess relatively high glass transition temperature, (T_g) and high decomposition temperature (T_d). As a result of these properties, different functional groups can be introduced to these systems to get specific applications and to maintain their excellent properties.

1.8.1 Poly (arylene ether sulfone)

Poly (arylene ether sulfone)s, PAES are a class of amorphous polymers with high strength and stiffness, long-term stability, and excellent resistance to acids, bases, hydrolysis, and oxidation, with a sulfone group in the backbone of the polymer.

The first commercially available PAES was introduced by Union Carbide Corp. in 1965. This polymer has a relative high glass temperature ($T_g = 190\ {}^0C$) which could be due to the presence of rigid aromatic structure along with a very polar sulfonyl group and may be due to varying bisphenol unit. PAES can be synthesized using either an electrophilic aromatic substitution (EAS) or the nucleophilic aromatic substitution (NAS) polycondensation reaction.
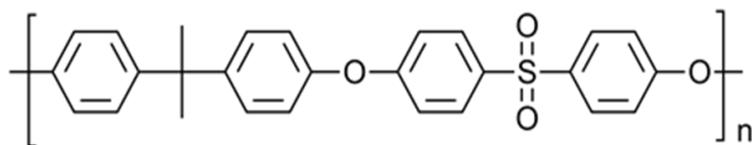
Figure 17. General stucture of a commercial poly (arylene ether sulfone), Udel (Union Carbide)

Radel was introduced by Union Carbide in the late 1970s, and it displayed good performance in thermal properties with $T_g = 220\ {}^0C$.[23] In 1972, Victrex was commercially introduced by ICI and it has a $T_g = 230\ {}^0C$. These PAES are amorphous thermoplastics with excellent thermal stability.
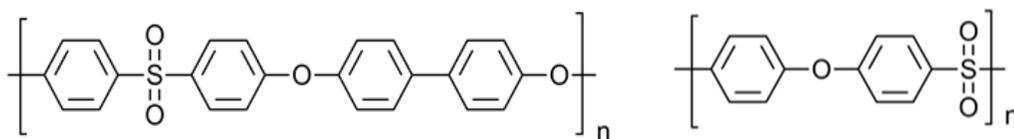
Figure 18. Radel (Union Carbide), (Left) and Victrex (ICI), (Right).

Thermal properties of PAEs can be tailored by changing the components in the backbone of the polysulfone.

1.8.2 Poly (ether ether ketone)s, PEEK

Poly (ether ether ketone), PEEK is a semicrystalline polymer and is used commonly in electronics, automobile, and aerospace technology. In 1978, ICI introduced PEEK, which is a PAE with a ketone group in the polymer backbone.[23] Commercially available PEEK has a $T_g = 145\,^0C$.
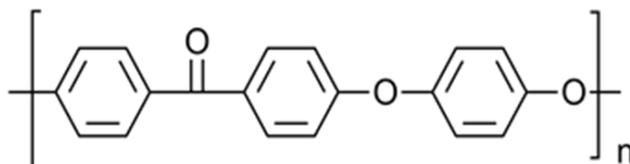
Figure 19. PEEK (ICI), $T_g = 145\,^0C$.

The series includes polymers such as poly(ether ketone), PEK and poly(ether ether ketone ketone), PEEKK. All have highly aromatic backbones and display high thermal stability.

1.8.3 Poly-(2,6-dimethyl-p-phenylene ether)

The simplest, commercially available PAE is poly-(2,6-dimethyl-p-phenylene ether), PPO. Its structure includes a highly aromatic backbone which contributes to its high temperature resistance, and tensile strength. It is an amorphous polymer with a $T_g = 215\,^0C$.[24]
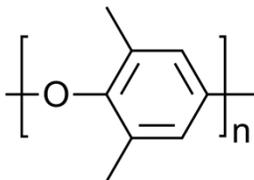
Figure 20. Poly-(2,6-dimethyl-p-phenylene ether) (PPO).

1.9 Polymerization via Nucleophilic Aromatic Substitution (NAS):

The polymers can be synthesized via a Nucleophilic Aromatic Substitution (NAS) polymerization. In NAS reaction, a nucleophile (Nu⁻) substitutes a good leaving group, usually a halide on the activated benzene ring. The aromatic ring is activated by strong electron-withdrawing group (EWG) located on the ortho or para position. When a halide group is attached ortho or para to an electron withdrawing group on a benzene ring, the ring will become activated towards NAS chemistry. A partial positive charge is formed on the ipso carbon, which is then susceptible to attack by a nucleophile.

X = F, Cl
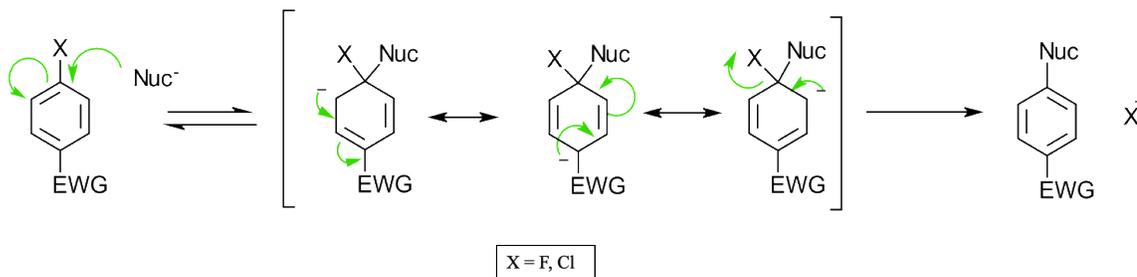
Scheme 1. NAS reaction mechanism.

As shown in the **Scheme 1**, the mechanism involves the attack at the electrophile by the nucleophile, aromaticity is broken to form a resonance-stabilized anion known as a Meisenheimer complex. This step is slow and the rate determining step. The second step occurs when the negative charge on the ring pushes out the leaving group. Aromaticity is restored once the leaving group is eliminated from the ring.[25]

TADF chromophores may be designed to resemble monomers for NAS polymerization (**Scheme 1**) and therefore may be easily incorporated into a PAE backbone. High thermal stability, excellent mechanical properties and solution processibilty of PAEs would make for excellent materials in a polymer OLED device. The incorporation of TADF molecules into PAE may prevent aggregation and self-

quenching, and as a result increase the thermal stability and would prolong the device lifetime.

1.10 Functionalization of PAE

Functional groups can be introduced into polymers to obtain desired physical and chemical properties. PAEs can be functionalized to get specific applications for example PAE may be sulfonated to make proton exchange membrane for fuel cells. Amination of PAEs give anionic exchange membrane for fuel cells. Incorporation of a chromophore in PAEs lead to the formation of polymer OLED. The TADF units may be incorporated into the backbone system via two different methods: pre-functionalization and post-functionalization **(Scheme 2).**
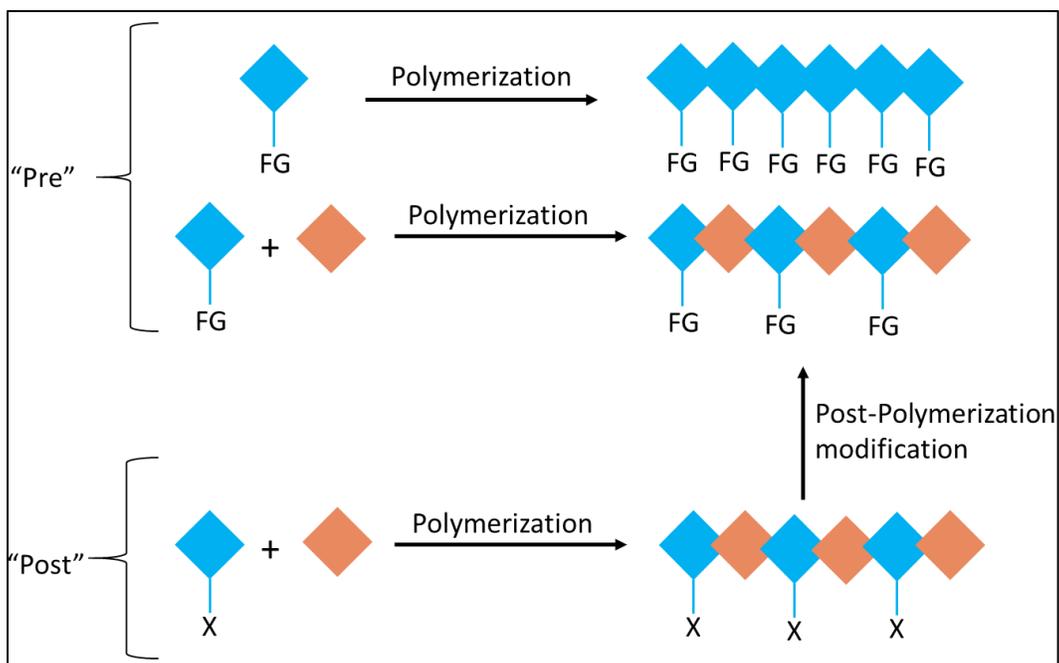
Scheme 2. "Pre" and "Post" Functionalization Methods.

In a pre-functionalization method, the monomers units are modified before polymerization with the donor group (FG). The modified monomers are then polymerized to give a functionalized polymer (TADF emitter). This method is suitable for functional groups that are capable of surviving polymerization conditions. In a post-functionalization method, the functional group (FG) is introduced at the polymer stage, also known as post-modification. After polymerization has occurred, the temporary functional group will be removed and the desired FG will be attached to the system. In the post-functionalization method, it is possible to attach a variety of different donor groups in one polymer base without having to synthesize various monomers.

1.11 Previous Work

Previous research work with the polymer OLED, using PAE system began with Jesse L. Picker's[26] work, by functionalizing iodinated 3,5-difluorodiphenyl sulfone monomer by using carbazole as the donor group. The first group of polymers synthesized was a continuation of work done by the Tatli. It was found that the polymerization of iodinated 3,5-difluorodiphenyl sulfone could be performed without displacing the iodine.[26] Picker attempted to post-functionalize the polymerized 3,5-DFDPS-I unit by substituting the iodo group with carbazole and other donors in a copper catalysed C-N coupling reaction. But this "post"method was unsuccessful due to possible crosslinking of the polymer chains at the previous C-I position.[27] The pre-functionalization method was attempted and 3,5-DFDPS-CBZ monomer was synthesiz by displacing iodo group with carbazole.
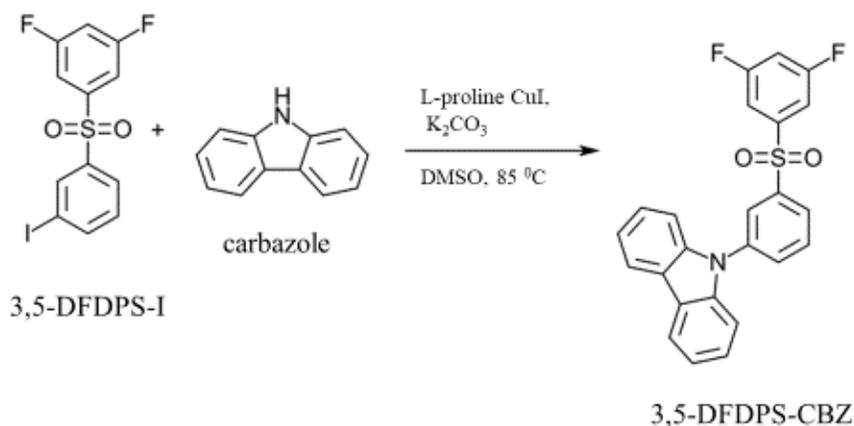
Scheme 3. Synthesis of Picker's 3,5-DFDPS-CBZ monomer.

The carbazole monomer was successfully incorporated into the polymer with bisphenol-A (BPA) and 4,4'-difluorodiphenyl sulfone (DPS). The carbazole donor group was used to achieve a wavelength close to the blue emission range and that could later be incorporated into a PAE system (see **Scheme 4).** Later various copolymers were synthesized using this method in which the polymer kept their themal stability high and polymer films showed broad emission from 370-600 nm with the peak emission occuring around 430 nm.
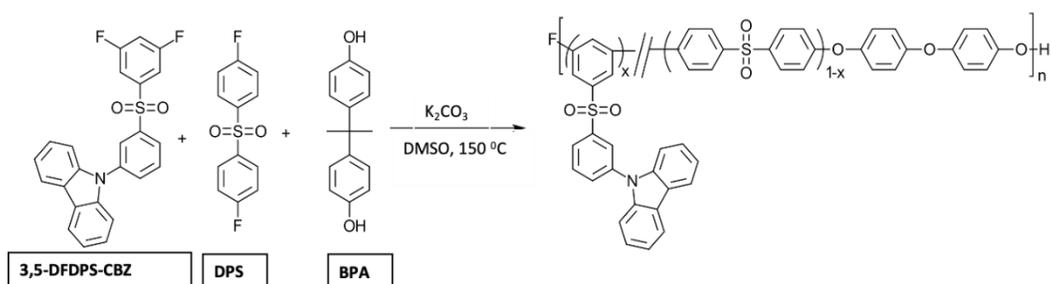
Scheme 4. Incorporation of 3,5-DFDPS-CBZ monomer into a PAE system.

Meyer[28], continued research in synthesis of diphenyl sulfone based chromophore using Cu and Pd based catalysts by varying the donor group on the

pendent pheny group, in order to get pure blue emission. The pre-functionalization method was used to synthesize various TADF chromophores, based on 3,5-difluorodiphenyl sulfone as an acceptor group functionalized with phenoxazine, carbazole, and indole donor groups **(Scheme 5).**
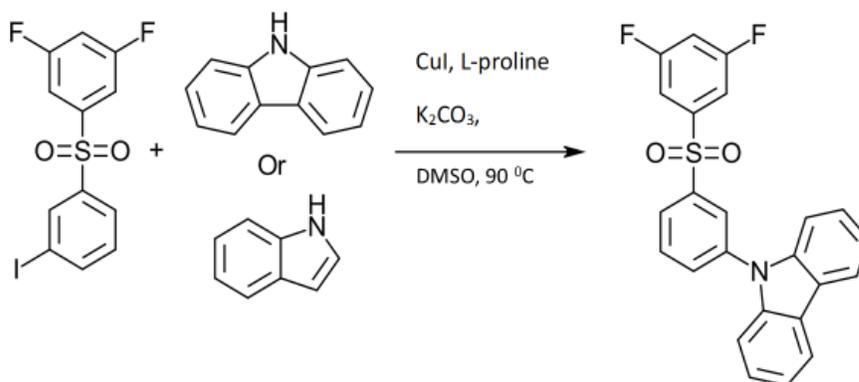
Scheme 5. Functionalization of 3,5-difluorodiphenyl sulfone.

Various monomers synthesized included 3,5-difluorodiphenyl sulfone-iodo (DFDPS-I) with carbazole, 3,5-difluorodiphenyl sulfone-iodo with 9-indole (DFDPS-IND), and 3,5-difluorodiphenyl sulfone-iodo with phenothiazine units.
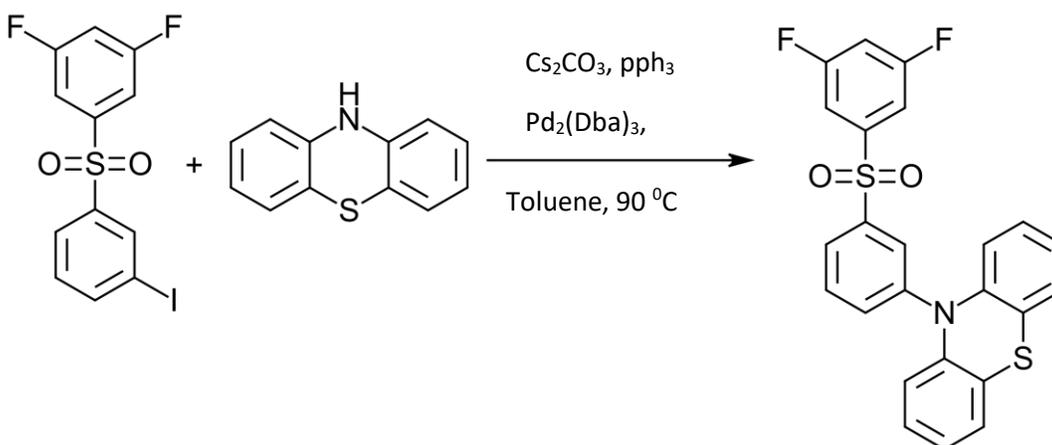
Scheme 6. Synthesis of 3'-(9-phenothiazine) 3,5-difluorodiphenyl sulfone.

The chromophores showed strong absorption at wavelengths between 290 nm and 340 nm. Polymerization of these monomers was successfully performed with bis-(4-fluorophenyl)phenyl phosphine oxide (dFTPPO) and 4,4'-dihydroxydipenyl ether via NAS reaction. Thermal analysis showed that each polymer had sufficiently high T_g values above 180^0C. In solution all copolymers showed strong and weak absorptions between 292 nm and 340 nm. Fluorescence spectra showed discrete, but broad emission peaks between 430 nm to 450 nm.

1.12 Current Work

The main goal of this project was to design and synthesize PAE-based TADF emitter using a donor-π-acceptor system, for blue OLED (~450 nm). PAEs are synthesized by nucleophilic polycondensation of 4,4'-difluorodiphenyl sulfone (DFDPS) with a 4,4'-bisphenol such as bisphenol-A (BPA). As a result, a linear polymer with all monomer components in the backbone is formed. In order to achieve these polymeric structures, both "pre" and "post" functionalization methods were explored. Depending on the identity of halide group, chemistry can now be done at the monomer stage or during post-polymerization functionalization. Since iodo groups show little reactivity in NAS reactions, the introduction of a halide in the monomer stage provides a site for further functionalization **(Scheme 7).**
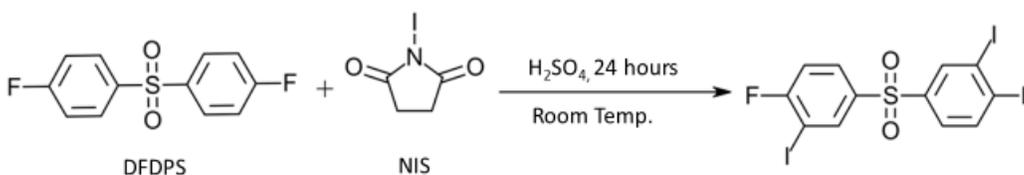
Scheme 7. Synthesis of di-iodo monomer.

Iodo has been chosen as an appropriate halide and will be installed using EAS mechanism. The iodo groups in the monomer present a highly twisted zig-zag

configuration.[19] Once iodinated, the monomer will be polymerized through the fluorine atoms. The co-monomers will be 4,4'-difluorodiphenyl sulfone (DFDPS) with bisphenol-A, serving as the nucleophilic reaction partner. These polymers will be fully characterized and then subjected to further functionalization.
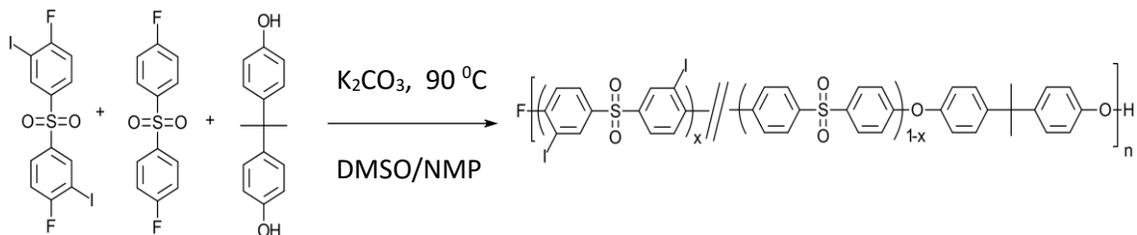
Scheme 8. Synthesis of copolymer using di-iodo monomer.

By using difluorinated monomer, polymerization through the fluorine atoms, post functionalization can be performed. Various donor groups can be incorporated into PAEs based copolymer with the C-I bond being the location for post-functionalization.

Carbazole   Phenoxazine

Indole   Phenothiazine
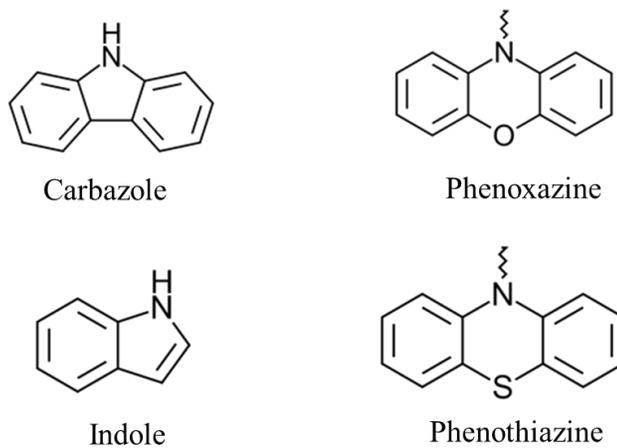
Figure 21. Various *N*-heterocyclic donors.

The primary goal of the project is to incorporate *N*-heterocyclic species, (carbazole, phenoxazine and phenothiazine), chosen as the donor unit to be attached

through the C-I bond to form the desired chromophores. With the donor group attached, the system will act as a "push-pull" compound where charge transfer is possible. By using DPS/BPA system high thermal stability and higher T_g values were expected. The ability to cast thin, smooth, transparent, flat films is analyzed with respect to changes in the concentrations of DFDPS-DI polymer. Finally, the development of a new blue (450 nm) TADF emitter with thermal stability, ease of processing, and long lifetime is expected as a result of this research.
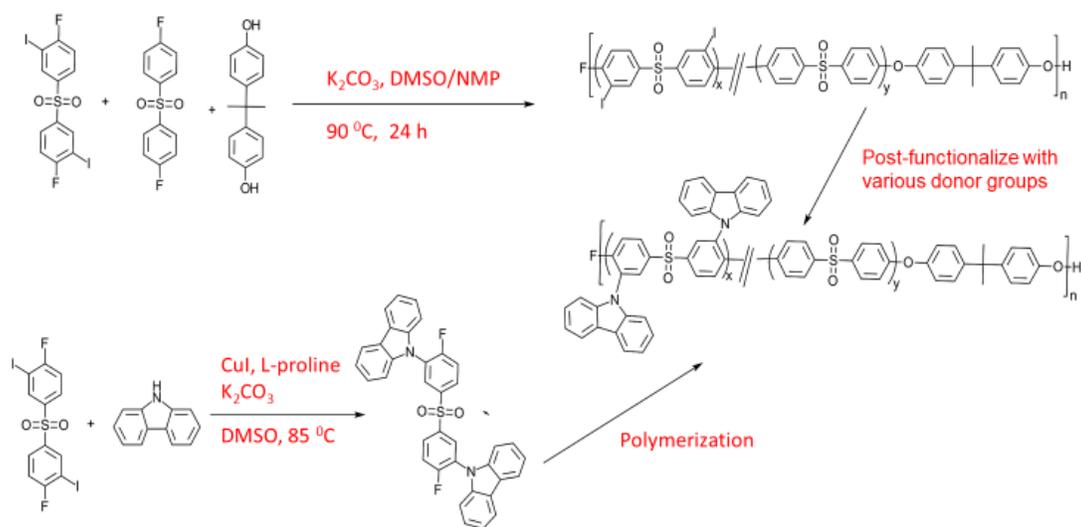
Scheme 9. Polymerization and incorporation of chromophore in DFDPS-DI monomer and polymer.

2. Experimental

2.1 Instrumentation/Characterization

GC/MS analyses were carried out using a Hewlett-Packard (HP) 6890 Series GC coupled with a HP 5973 Mass Selective Detector/Quadrupole system. A Bruker AVANCE 300 MHz Nuclear Magnetic Resonance (NMR) was used to acquire a ^{1}H and ^{13}C spectra. The instrument operates at 300 MHz (^{1}H) and 75.5 MHz (^{13}C) respectively. All compounds were dissolved in appropriate deuterated solvents (DMSO-d_6 or CDCl$_3$) at a concentration of ~ 30 mg/ 0.6 mL. Size Exclusion Chromatography (SEC) was performed using a system consisting of a Viscotek Model VE3580 Refractive Detector (IR) and Viscotek Model 270 Dual Detector (viscometer and light scattering). Two polymer Laboratories 5 µm PL gel Mixed C columns (heated to 35 ^{0}C) were used with tetrahydrofuran (THF) 5% (v/v) acetic acid as the eluent and a GPC max VE-2001 with pump operating at 1.0 mL/min. The IR signal (calibrated using polystyrene standards from Scientific Polymer Product, INC) was used to determine number average, Mn, and dispersity values. Thermogravimetric analysis (TGA) and Differential Scanning Calorimetry (DSC) were carried out on an TA Instruments TGA Q500 and DSC Q200 (under nitrogen or air), respectively, at a heating rate of 10 ^{0}C/ min. Fluorescence data was acquired using an Agilent Technologies Cary Eclipse Fluorescence Spectrophotometer and UV/Vis data was acquired using an Agilent Cary 50 UV/Vis Spectrometer. Melting points were determined using a MEL-TEMP instrument and are

uncorrected. Elemental Analyses were obtained from Midwest Micro Labs, Indianapolis, IN.

2.2 Materials

The compounds carbazole, L-proline, copper (l) iodide (CuI), potassium carbonate, hydrochloric acid, chloroform-d (CDCl$_3$), dimethyl sulfoxide-d_6 (DMSO-d_6), N-methylpyrrolidinone (NMP), m-cresol, phenothiazine, indole, and 2-naphthol were purchased from Sigma Aldrich. L-proline, phenothiazine, chloroform-d (CDCl$_3$), dimethyl sulfoxide-d_6 (DMSO-d_6), carbazole, and HCl were used as received. DMSO and NMP were dried over CaH$_2$ and distilled under nitrogen prior to use. Potassium carbonate and cesium carbonate were dried in an oven at 130 ^{0}C. CuI was activated by washing in a Soxhlet extractor using tetrahydrofuran (THF), using the procedure described by Kohnen and coworkers.[29] The compound bis-(4-fluorophenyl) sulfone (DPS) was purchased from Oakwood Chemicals and used as received. Tetrahydrofuran (THF), and magnesium sulfate were purchased from Fisher Chemical and used as received. Ethanol was purchased from Decon laboratories and used as received. Chloroform was purchased from EMD Millipore Corp and was used as received. Bisphenol-A was purchased from Sigma Aldrich Chemical Co. N-iodosuccinimide (NIS) was purchased from Acros Organics and used as received. Sulfuric acid (H$_2$SO$_4$) was purchased from BDH.

2.3 Synthesis of DI-DFDPS monomer (3),[19]

To a 50 mL round- bottomed flask, equipped with a stir bar and nitrogen gas inlet, were added DFDPS (2.00 g, 7.89 mmol), NIS (4.42 g, 19.7 mmol), and H$_2$SO$_4$ (15 mL). The reaction mixture was stirred vigorously at room temperature for 24 hours. GC/MS analysis of an aliquot sample showed that the reaction mixture contained 87%

Of the desired di-iodo species. The reaction mixture was precipitated from ~500 mL vigorously stirred water and the resulting solids were isolated using vacuum filtration. The resulting white powdered solid was washed first with water and then with 200 mL of hexane followed by recrystallization from toluene. The crystals were separated by vacuum filtration. GC/MS analysis indicated 97% purity of desired di-iodo product, DI-DFDPS monomer. The melting point was determined to be 196 – 198 ^{0}C. Elemental analysis: Calculated: C- 28.59 %; H- 1.5 %; Found: C- 28.61 %, H- 1.40 %.

^{1}H NMR (CDCl$_3$; δ): 7.2 (dd,1H), 7.91 (m, 1H), 8.4 (dd,1H). ^{13}C NMR (CDCl$_3$; δ): 80.2 (dd), 118 (d), 130 (s), 138 (s), 139 (s), 164.5 (d).

2.4 "Pre" Functionalization of DFDPS-DI Monomer + CBZ

Into a 25 mL Schlenk flask, equipped with a stir bar and nitrogen gas inlet were added DFDPS-DI monomer (0.250 g, 0.4940 mmol), carbazole (CBZ) (0.205 g, 1.22 mmol), activated CuI (0.0112 g, 12 mol %), L-proline (0.0169 g, 30 mmol %), and K$_2$CO$_3$ (0.2302 g, 1.67 mmol) . The Schlenk flask was evacuated and backfilled with nitrogen and DMSO (0.4 mL) was added. The resulting mixture was stirred at 90 ^{0}C for 36 hours. The GC/MS result showed some traces of mono substituted product (one I was replaced with CBZ) but it did not show the formation of any di substituted product at all. After 56 hours run, the GC/MS was run again, it again didn't show the formation of di-substituted product at all.

2.5 Model Reaction: DFDPS-DI Monomer(3) with p-cresol(5),

To a 10 mL round-bottomed flask, equipped with astir bar, a condenser and a nitrogen inlet were added DFDPS-DI monomer (0.075 g, 0.148 mmol),p-cresol (0.0694 g, 0.415 mmol), K$_2$CO$_3$ (0.0450 g, 0.326 mmol), DMSO (0.2 mL), and NMP (0.1 mL). The reaction mixture was heated to 90 ^{0}C for 24 hours. The reaction mixture was added dropwise to a beaker of vigorously stirred DI water and the resulting

solids were isolated via vacuum filtration and dried to afford 0.041 g (55 % yield) of the desired compound. ^{1}H NMR (CDCl$_{3;}$ δ): 6.73 (d, 1H), 6.95 (d, 1H), 7.21 (d, 1H), 7.76 (dd, 1H), 8.36 (d, 1H). ^{13}C NMR (CDCl$_{3;}$ δ): 20.9 (s), 87.4 (s), 115,9 (s), 120.2 (s), 129.2 (s), 130.8 (s), 135.4 (s), 136.5 (s), 140.4 (s), 152.3 (s), and 161.9 (s).

2.6 Synthesis of DI-Copolymers, (9a-b)

The procedure for polymer **9b** is provided as an example.

To a 10 mL round-bottomed flask, equipped with a stir bar and a condenser with a nitrogen gas inlet, were added DFDPS-DI monomer (0.144 g, 0.280 mmol), Bisphenol-A (0.260 g, 1.14 mmol), DFDPS (0.222 g, 0.873 mmol), K$_2$CO$_3$ (0.485 g, 3.51 mmol), DMSO (1.5 mL), and NMP (0.7 mL). Using a silicon oil bath and a thermocouple hotplate, the reaction mixture was heated to 90 ^{0}C for 24 hours. The reaction mixture was added dropwise to a beaker of ~ 500 mL vigorously stirred DI water and the resulting solids were isolated via vacuum filtration. The polymer was then dissolved in approximately 3 mL of THF and precipitated from ~ 300 mL vigorously stirred water, and the polymer was isolated by vacuum filtration, followed by drying in the drying pistol until constant mass to afford 0.178 g (~ 95.1%) of the desired polymer **9b**. A small sample was utilized for 1H NMR spectroscopy and GPC/SEC analyses, which both indicating that the polymerization took place.

^{1}H NMR (CDCl$_{3;}$ δ): 1.7 (s), 6.79 (d), 6.95 (d), 7.05 (d), 7.25 (d), 7.79 (dd), 7.81 (d), 8.36 (d). ^{13}C NMR (CDCl$_{3;}$ δ): 31.2 (s), 42.4 (s), 87.5 (s), 116.4 (s), 117.7 (s), 119.8 (s), 128.4 (s), 128.6 (s), 129.3 (s), 129.7 (s), 135.4 (s), 139.1 (S), 147.1 (s), 152.6 (s), 152.8 (s), and 162.0 (s).

The other polymer **9a** (10% 0f **3**)**,** 0.2 g (87.7%) was synthesized using the same method, only with different ratios of the reactants.

2.7 Post-Functionalization with carbazole(4), 10a-b

The procedure for polymer **10b** is provided as an example.

To a 10 mL round-bottomed flask, equipped with a stir bar, a condenser and a nitrogen inlet, were added **9b** (0.150 g, 0.297 mmol), carbazole (0.0320 g, 0.2964 mmol), K_2CO_3 (0.174 g, 1.26 mmol), activated CuI (0.0016 g, 12mol%), L-proline (0.0025 g, 30 mol%), 1.0 mL of distilled DMSO and 0.5 mL of distilled NMP. The flask was heated in an oil bath at 90 ^{0}C for approximately 24 hours.

The reaction mixture was added dropwise to approximately 500 mL DI water with vigorous stirring and left to stir for approximately 3 hours. The resulting solids were isolated via vacuum filtration and the product was left to dry over the vacuum overnight. The precipitate was stirred with approximately 200 mL ethanol for about 2 hours and the solids were isolated via vacuum filtration and the product was left to dry overnight. The final yield was 0.09 g (~ 69.7%) of the desired polymer. ^{1}H NMR (CDCl$_3$; δ): 6.65 (d), 6.95 (d), 7.01 (d), 7.2 (d), 7.28 (d), 7.85 (d), 8.05 (d), 8.16 (d). ^{13}C NMR (CDCl$_3$; δ): 31.0 (s), 42.6 (s), 109.8 (s), 117.7 (s), 118.9 (s), 119.4 (s), 119.8 (s) 120.3 (s), 123.6 (s), 126.1 (s), 127.9 (s), 128.5 (s), 128.8 (s), 129.7 (s), 130.2 (s), 135.4 (s), 140.4 (s), 147.2 (s), 152.3 (s), 152.9 (s), 158.3 (s), and 162.0 (s).

The other polymer **10a** (10% 0f **9**), 0.15 g (81 %) was synthesized using the same method, only with different ratios of the reactants.

2.8 Post-Functionalization with phenoxazine(11), 12a-b

The procedure for polymer **12b** is provided as an example.

To a 10 mL round-bottomed flask, equipped with a stir bar, a condenser and a nitrogen inlet, were added 25% **9b** (0.150 g, 0.297 mmol), phenoxazine (0.0679 g, 0.3709 mmol), K_2CO_3 (0.174 g, 1.26 mmol), activated CuI (0.0016 g, 12mol%), L-proline (0.0025 g, 30 mol%), 1.0 mL of distilled DMSO and 0.5 mL of distilled NMP. The flask

was heated in an oil bath at 90 ^{0}C for approximately 24 hours.

The reaction mixture was added dropwise to approximately 500 mL DI water with vigorous stirring and left to stir for approximately 3 hours. The resulting solids were isolated via vacuum filtration and the product was left to dry over the vacuum overnight. The precipitate was stirred with approximately 200 mL ethanol for about 2 hours and the solids were isolated via vacuum filtration and the product was left to dry overnight. The final yield was 0.1674 g (~91.58%) of the desired polymer. ^{1}H NMR (CDCl$_3$; δ): 1.52 (s), 6.1 (s), 6.51 (s), 6.9 (dd), 7.3 (d), 7.9 (d). ^{13}C NMR (CDCl$_3$; δ): 3.9 (s), 42.4 (s), 107.5 (s), 113.5 (s), 135.0 (s), 117.6(s), 120.1 (s), 121.1 (s), 123.2 (s), 125.7 (s), 128.6 (s), 129.7 (s), 131.9 (s), 134.1 (s), 135.4 (s), 138.0 (s), 143.9 (s), 147.4 (s), 149.9 (s), 152.7 (s), 155.8 (s), and 162.2 (s).

The other polymer **12a** (10% 0f **9**), 0.2 g (99.0%) was synthesized using the same method, only with different ratios of the reactants.

2.9 Post-Functionalization with Indole(13), 14a-b

The procedure for polymer **14b** is provided as an example.

To a 10 mL round-bottomed flask, equipped with astir bar, a condenser and a nitrogen inlet, were added **9b** (0.2 g, 0.396 mmol), phenoxazine (0.0464, 0.2535 mmol), K$_2$CO$_3$ (0.186 g, 1.35 mmol), activated CuI (0.0022 g, 12mol%), L-proline (0.0034 g, 30 mol%), 1.5 mL of distilled DMSO and 0.7 mL of distilled NMP. The flask was heated In an oil bath at 90 ^{0}C for approximately 24 hours.

The reaction mixture was added dropwise to approximately 1000 mL DI water with vigorous stirring and left to stir for approximately 3 hours. The resulting solids were isolated via vacuum filtration and the product was left to dry over the vacuum overnight. The precipitate was stirred with approximately 200 mL ethanol for about 2 hours and the

solids were isolated via vacuum filtration and the product was left to dry overnight. The final yield was 0.1476 g (~ 74.5%) of the desired polymer. ^{1}H NMR (CDCl$_3$; δ): 1.65 (s), 6.65 (d), 6.84 (d), 6.90 (d), 6.94 (d), 7.01 (d), 7.08 (d), 7.10 (dd), 7.16 (dd), 7.25 (d), 7.32 (d), 7.63 (d), 7.86 (d), and 8.08 (d). ^{13}C NMR (CDCl$_3$; δ): 31.1 (s), 43.6 (s), 100.1 (s), 104.2 (s), 112.4 (s), 117.7 (s), 119.3 (s), 119.9 (s), 120.9 (s), 122.7 (s), 123.9 (s), 127.7 (s), 128.4 (s), 129.7 (s), 130.5 (s), 135.4 (s), 136.3 (s), 140.6 (s), 147.1 (s), 148.4 (s), 151.6 (s), 152.8 (s), 156.5 (s), and 162.1 (s).

The other polymer **14a** (10% 0f **9**), 0.2 g (97 %) was synthesized using the same method, only with different ratios of the reactants.

2.10 Characterization

2.10.1 Nuclear Magnetic Resonance (NMR) Analysis

The NMR spectra were acquired using a Bruker AVANCE 300 MHz Instrument. All the polymer samples (~ 35 mg) were dissolved in Chloroform-d_6. ^{13}C NMR data was acquired overnight, 15 hours (15000 scans), while DEPT-90 ^{13}C NMR data was acquired for 4 hours (4,096 scans). The monomer samples (~ 30 mg) were dissolved in Chloroform-d_6. ^{13}C NMR data was acquired overnight, 15 hours (15000 scans), while DEPT-90 ^{13}C NMR data was acquired for 30 min (1024 scans).

2.10.2 Absorption and Emission Spectra

The UV/Vis absorption and fluorescence spectra of polymers were acquired from 20 Micromolar (μM) solution in THF and 5% (v/v) acetic acid THF solution.

2.10.3 Thermogravimetric Analysis (TGA)

The thermal stability of the polymers under nitrogen and air was investigated using a TA Instruments Q500 Thermogravimetric Analyzer. The method involved heating ~ 6 mg of sample at a rate of 10 ^{0}C/min from 40^{0}C to 800^{0}C, under nitrogen or an air atmosphere. The weight loss was recorded as a function of time and the thermal stability was reported as 5% weight loss ($T_{d-5\%}$).

2.10.4 Differential scanning Calorimetry (DSC)

A TA Instruments, Q200 Differential Scanning Calorimeter was used to investigate any thermal transition of the polymers. The sample was placed in a Tzero aluminum pan and analyzed using a method that involved heating at 10 ^{0}C/min from 40 ^{0}C to 250 ^{0}C and cooling at 20 ^{0}C to 40 ^{0}C in two cycles under a nitrogen atmosphere. The first heating cycle was utilized to erase the thermal history of the polymers while the glass transition temperatures, T_g, was determined by finding the midpoint of the tangent of the change in baseline of the second heating cycle.

3. RESULTS AND DISCUSSION

3.1 Outline of the Project

The main goal of this project was to explore "Pre" and "Post" functionalization routes to synthesize PAE-based blue (~ 450 nm) TADF emitters modeled on donor-π-acceptor systems. PAE systems are an excellent choice for functionalization due to their good thermooxidative as well as physical properties.[30] The functional groups can be introduced prior to ("Pre") or after ("Post") polymerization is completed. Both routes have been used to modify polymers to enhance their properties and act as access points to further modification chemistries.[31] Depending on the identity of halide groups, chemistry can now be done at the monomer stage or during post-polymerization functionalization. Since iodo groups typically show little reactivity in NAS reactions, the introduction of an iodo group at the monomer stage provides a site for further functionalization **(Figure 22).**
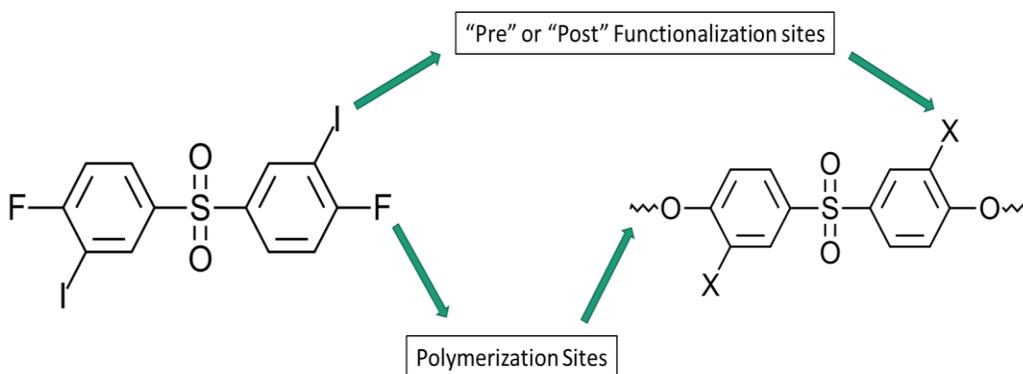
Figure 22. Functionalization and Polymerization sites in DI-DFDPS monomer.

Fluorine atoms provide sites for polymerization and allow for convenient incorporation of the TADF chromophore, or its precursor, into a PAEs backbone via

NAS reactions. Iodo groups have been chosen as an appropriate halide and will be installed using EAS reaction, which should place them at the *ortho*-position, relative to the ether bond in the backbone.

Once iodinated, the monomer will be polymerized as a component in a series of PAEs, of varying composition, to demonstrate control of the number and placement of functional groups.

3.2 Synthesis of DI-DFDPS Monomer, 3

The diiodo-difluorodiphenyl sulfone monomer (DI-DFDPS), **3,** was synthesized by iodination of 4,4'-(difluorodiphenyl) sulfone, **1,** using *N*-iodosuccinimide (NIS) via an EAS reaction **(Scheme 10).** The reaction was conducted in concentrated sulfuric acid as a solvent and catalyst at room temperature, giving diiodo compound **3**.[19] The compound **1** and NIS (**2**) were combined in a 1:2 molar ratio.
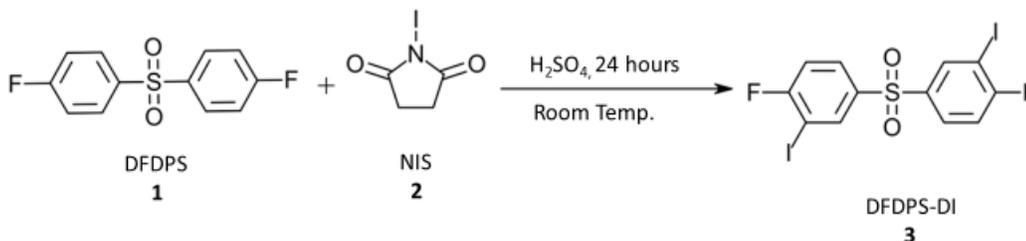
Scheme 10. Synthesis of DI-DFDPS monomer (**3**) via EAS.

The reaction was run at room temperature for 24 hours at which point GC/MS analysis determined there was ~ 87% conversion to the desired di-iodo product with some mono-iodo and tri-iodo products also present. The reaction mixture was poured into a large excess of water and the resulting solids were isolated via vacuum filtration. Compound **3** was washed with water first and then with 200 mL of hexane, followed by recrystallization from toluene. The crystals were separated by vacuum filtration at which point GC/MS analysis indicated 97% purity of **3**. The melting point was 196 – 198 ^{0}C

and the structure of **3** was confirmed via GC/MS, elemental analysis, and NMR spectroscopy. The ^{1}H NMR and ^{13}C NMR spectra are shown in **Figure 23** and **Figure 24**, respectively.
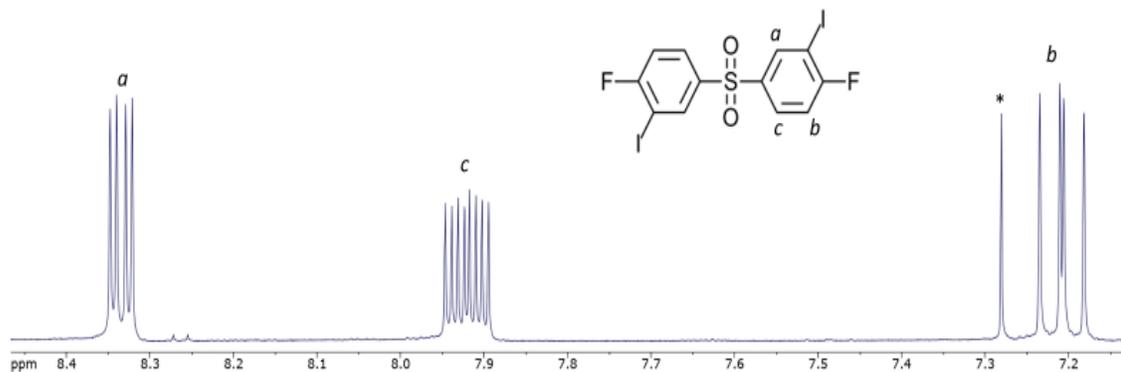
Figure 23. 300 MHz ^{1}H (CDCl$_3$) NMR spectrum of **3** (* indicates CHCl$_3$).

The 300 MHz ^{1}H spectrum of **3** shows 3 unique hydrogen peaks. Protons *a* appear at 8.35 ppm as a doublet of doublets due to *meta* coupling with fluorine and proton **c**. Protons **b** appear at 7.2 ppm as a doublet of doublets due to *ortho* coupling with fluorine and proton **c**. Protons *c,* at 7.93 ppm, appear as a doublet of doublet of doublets due to *ortho* coupling with proton *b*, and *meta* coupling with fluorine and proton *a*.

The 75.5 MHz ^{13}C (CDCl$_3$) NMR spectrum of **3** shows 6 unique carbon peaks. The carbon *a*, at 165 ppm, is a doublet with a large coupling constant (~250 Hz) for the ipso-fluorine atom. Carbon atoms *f* and *b* appear as doublets, at 118 ppm and 82 ppm, respectively due to the coupling with the *ortho* fluorine. Carbon atoms *c* and *e*, *meta* to the fluorine appear doublets at 130.5 ppm and 138.5 ppm, respectively. Quaternary carbon *d* is *para* to the C-F group and appears as a doublet at 139 ppm.
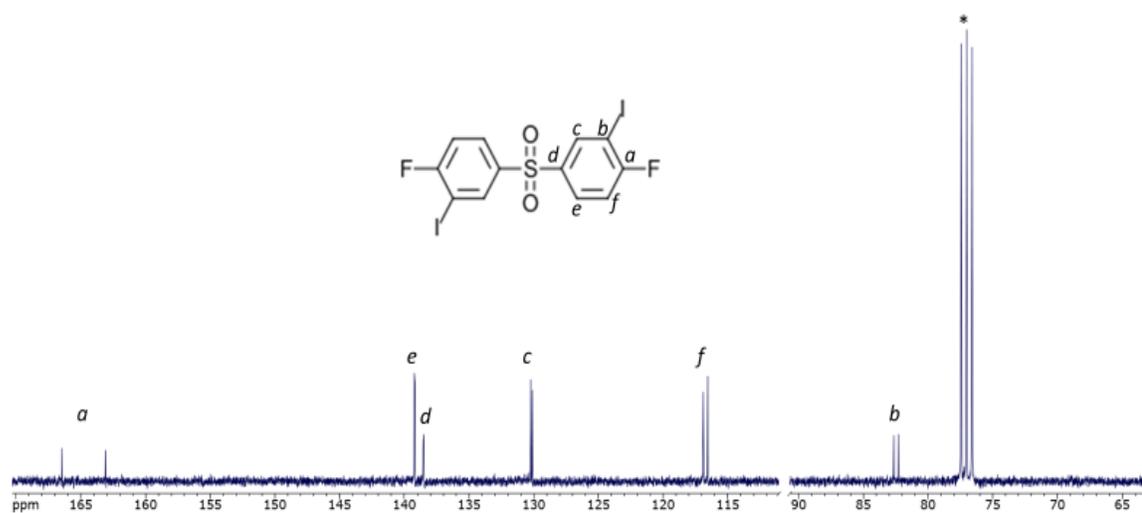
Figure 24. 300 MHz ^{13}C (CDCl$_3$) NMR spectrum of **3** (* indicates CHCl$_3$).

3.3 Routes to functionalize the Polymers

"Pre" Functionalization: Synthesis of chromophore (DI-DFDPS+CBZ)

To synthesize the polymers, two different approaches "Pre" and "Post" functionalization were attempted. The first method was to synthesize a chromophore via the "Pre" method, but this approach was not very successful (see **Scheme 11**). In the "Pre" method, monomer **3** was reacted with different donor groups, like carbazole and indole, in the presence of a copper catalyst, however, very little conversion to the desired material was observed. For example, in the reaction with carbazole, a variety of different compounds were observed but the desired compound, **4a,** was not present in any appreciable amounts. In the modification reaction with indole, some of the fluorine atoms were clipped off instead of the iodo group being substituted. In fact, at least four unique products were observed in GC/MS analyses of the reaction mixtures. The postulated structures of these different compound, which match with the molecular weights observed in GC/MS data, are given in **Scheme 11**. Because of the difficulties in preparing the desired "Pre" chromophores this approach was abandoned.

38
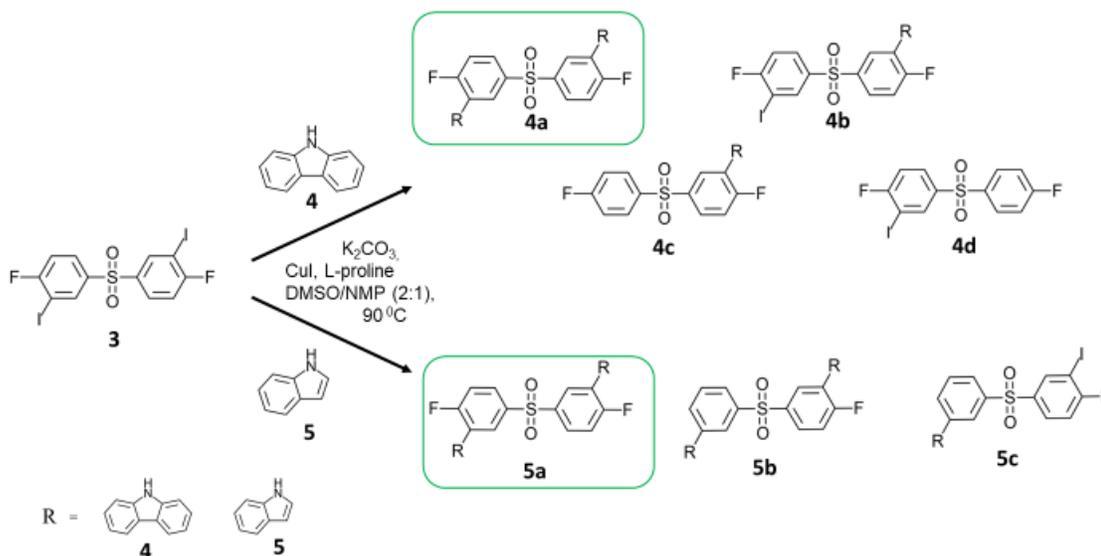
Scheme 11. "Pre" modification route; DI-monomer with CBZ and Indole.

The second approach was to prepare chromophore containing polymers via the "Post" method. The polymers, containing iodo groups were synthesized using monomer **3** and various co-monomers (bisphenol-A, as the nucleophilic component and DFDPS, as the co-monomer, electrophilic component) to achieve a copolymer. The desired functional groups were attached to the monomer after polymerization. Polycondensation reactions were performed using typical NAS conditions.

3.4 Model Reaction: "Post" functionalization of monomer 3,

A model reaction, using *p*-cresol as the nucleophile, was carried out to determine if the iodo group would be stable under typical NAS conditions, thus providing a pathway for post-functionalization modification reactions. In addition, the product of the model reaction would provide a platform to determine the optimal conditions for C-N coupling reactions to be performed on the corresponding polymers. The reaction of DI-DFDPS monomer **3** and *p*-cresol (**6**) was performed in the presence of K_2CO_3, in DMSO/NMP

39

(2:1) at 90 ^{0}C for 24 hours **(Scheme 12).** The reaction progress was monitored via ^{1}H NMR spectroscopy until the spectra showed complete conversion (see **Figure 25**).
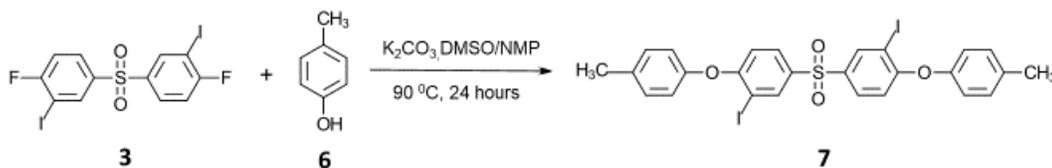
Scheme 12. Model Reaction (DI-monomer **3** + p-cresol).

The reaction mixture was precipitated from vigorously stirred DI water and the resulting solids were isolated via vacuum filtration and dried to afford 0.041 g (54.6% yield) of the desired compound. The structure of **7** was confirmed by its ^{1}H and ^{13}C (CDCl$_3$) NMR spectra as shown in **Figure 25 and 26,** respectively. These spectra confirmed that the fluoro groups on the structure served as the leaving groups while the iodo groups were undisturbed under the NAS conditions.
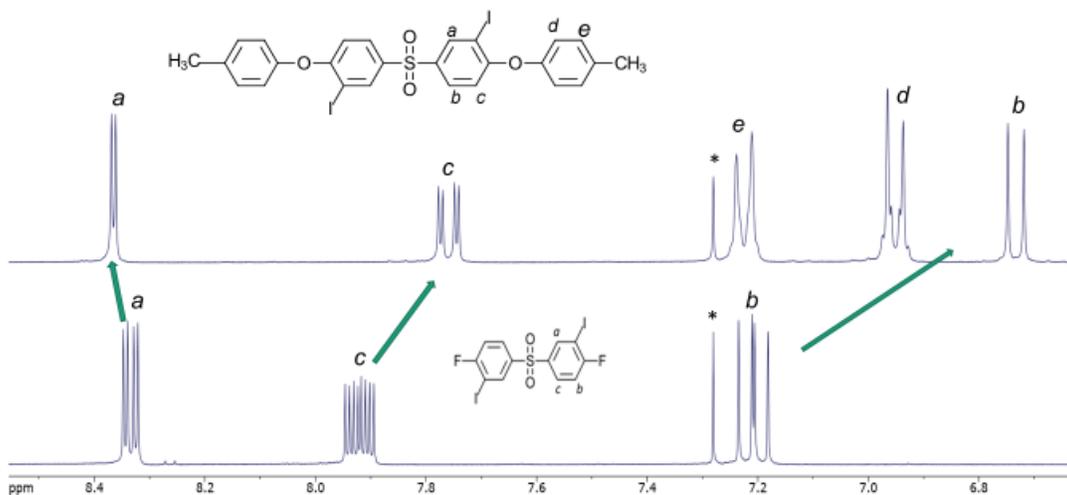
Figure 25. 300 MHz ^{1}H (CDCl$_3$) spectrum of **7** (* indicates CHCl$_3$).

The 300 MHz ^{1}H (CDCl$_3$) spectrum of **7** shows 5 unique hydrogen peaks and support successful incorporation of *p*-cresol via substitution of the two fluoro groups and with iodine undisturbed. The proton *a* appears as doublet at 8.37 ppm due to *meta*

40

coupling with *c*. The proton *b* appears as a doublet at 6.74 ppm due to *ortho* coupling

with *c*. Proton *c* appears as a doublet of doublet at 7.78 ppm due to the *ortho* coupling

with *b* and *meta* coupling with *a*. The protons *d* appear as a doublet at 6.96 ppm due to

ortho coupling with *e* and *e* appears as doublet at 7.23 ppm due to *ortho* coupling with **d**.

The integration of proton **a** relative to *d* or *e* can be used to show successful fluorine

displacement and *p*-cresol substitution by observing 1:2 ratio of protons.
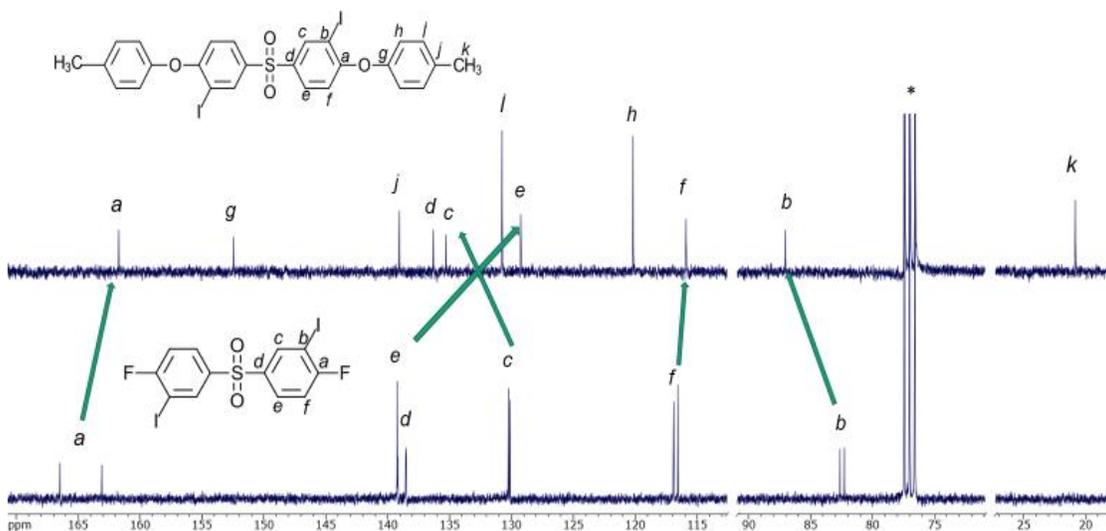
Figure 26. 75.5 MHz ^{13}C (CDCl₃) NMR spectral overlay of **3** and **7** (* indicates CHCl₃).

The 75.5 MHz ^{13}C (CDCl₃) NMR spectrum (**Figure 26**) of **7** shows 11 unique

carbon atoms peaks, with 5 new signals introduced from the substitution of the p-cresol

group. The overlay confirms the successful displacement of the fluoride groups in the

iodo monomer while maintaining the iodo group. The major changes in the spectrum are

the collapse of the doublets to singlets, which indicate the quantitative conversion to aryl

ether bonds. The new peaks, at 153 ppm (carbon atom *g*) and 162 ppm (carbon atom *a*),

which represent the carbon atoms of the C-O bonds, can be seen in the model product.

The most important feature of the spectrum is the presence of a carbon atom of the C-I

bond, present at 87.4 ppm, indicating that the iodo group was stable under the reaction

41

conditions and it should be possible to carry it, undisturbed, into the corresponding polymer.

These new carbons were labelled as *g, h, i, j,* and *k*. As was observed in monomer **3,** the signals *a, b, c, d, e,* and *f* appears as doublets due to the coupling with fluorine. These signals that were previously split by fluorine atoms in the **3** monomer, carbons *a −* *f,* now appear as singlets due to the successful displacement of the fluorine atoms with oxygen atoms.

3.5 Synthesis of DI-DFDPS-DPS/Bis-A copolymers, 9 a-b

The iodo copolymers, **9a-b,** were successfully prepared by the reaction of monomer **3** with 4,4'-difluorodiphenylsulfone (DPS, **1**) and bisphenol-A (BPA, **8**), in the solvent mixture DMSO/NMP (2:1) at 90 ^{0}C under NAS, polycondensation conditions.
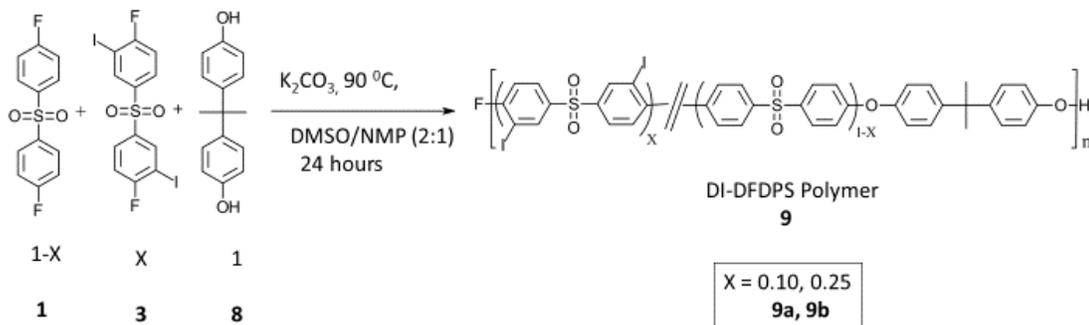
Scheme 13. Synthesis of DI-DFDPS-DPS/DPE copolymers, **9 a-b.**

Based off the time for the model reaction, after 24 hours the reaction material was precipitated from vigorously stirred DI water, and resulting solids were isolated via vacuum filtration. The reaction material was then re-precipitated by dissolving in THF and adding dropwise to an excess of DI water to remove any residual salts.

Monomer **8** was held constant and by varying the molar ratio of monomers **3** (x) and **1** (1-x) with regards to each other (10:90 and 25:75), two copolymers were

prepared where **x** = 0.10 and 0.25 for copolymers **9a** and **9b**, respectively (known as
10% and 25% DI, respectively). As was confirmed for the model reaction, the
polymerization occurred by the replacement of the fluorine atoms and the iodo groups
were successfully carried into the polymer under the standard NAS conditions. ^{1}H NMR
and ^{13}C (CDCl[3]) NMR analyses were used to determine the structure of polymers **9a-b**
and overlays of the ^{1}H NMR and ^{13}C (CDCl[3]) NMR spectra are shown in **Figure 27** and
Figure 28, respectively.
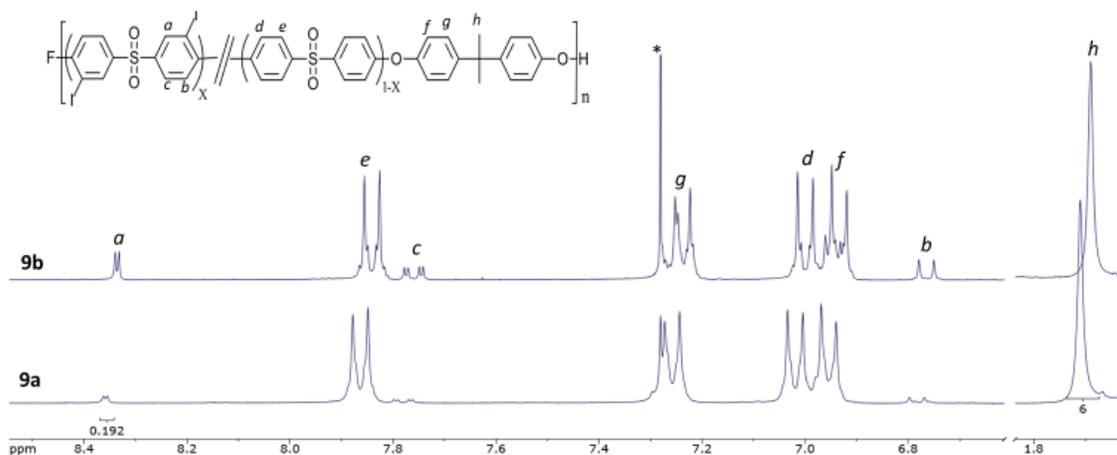
Figure 27. 300 MHz ^{1}H NMR spectral overlay of **9a** (10% DI) and **9b** (25% DI) (*
indicates CHCl[3]).

The 300 MHz ^{1}H NMR spectra of **9a** and **9b** show the successful incorporation
of **3** into a polymer containing DPS and BPA. The increasing concentration of monomer
3 in copolymers **9a** and **9b** is reflected by the increasing intensities of the proton signals
labelled *a*, *b*, and *c*. Protons *d* and *e* result from the DPS unit and appear at 7.88 ppm and
7.03 ppm. Protons *f* and *g* result from the BPA unit and appear at 6.93 ppm and 7.24
ppm. The ratio of bisphenol-A was held constant for both polymers and was used as the
standard for integration. The integration of the aromatic (proton *a*) and non-aromatic
protons (CH[3] groups, set at 6 H) confirmed that monomer **3** was incorporated in the

approximate feed ratio (0.10 and 0.25) for copolymers **9a** and **9b**. The polymer **9a** has an integration ratio of 0.2**:**6 (**a:h**) when integrating *a* relative to *h* which confirms the desired ratio of **3** has been incorporated into the polymer. If 100% of **3**, was used, then the ratio would be 2:6 (**a:h**), but only 10% was added, thus, 0.2**:**6. Similarly, copolymer **9b** has an integration ratio of 0.5**:**6 (**a:h**), when integrating *a* relative to *h*, which represents the successful incorporation of 25% of monomer **3** into the polymer backbone.

The 75.5 MHz ^{13}C (CDCl$_3$) NMR spectra (**Figure 28**) of polymers **9a-b** further supports the incorporation of **3** into a BPA and DPS polymer backbone system. It is confirmed that the carbon-iodo bond, present at 87.4 ppm, remained intact as shown in **Figure 28**. With the carbon-iodine bond carried into the polymer, a site for "Post" functionalization was successfully established.

The carbon signals that were previously split by fluorine atoms in the monomer **3**, now appear as singlets due to the successful substitution of fluorine atoms with ether bonds, and the subsequent loss of carbon-fluorine coupling. Furthermore, a new peak (*a*) appearing at 161.8 ppm shows the newly formed carbon-oxygen bond in the polymer backbone. The carbon atoms assigned to **3** can be observed to have increasing concentrations when comparing **9a** and **9b**. The carbon signals, *h* and *i*, corresponding to the DPS comonomer can be observed to slightly decrease from **9a** to **9b**, due to the increasing amounts of **3** present.
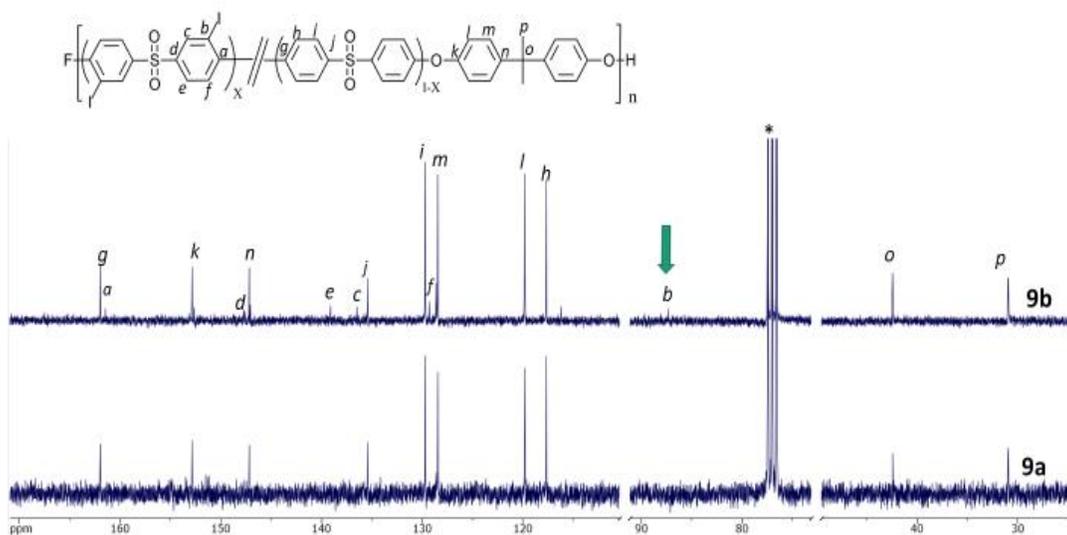
Figure 28. Overlay of 75.5 MHz ^{13}C (CDCl$_3$) NMR of **9a** and **9b** (* indicates CHCl$_3$).

Table 1. Monomer ratios, %yield, MW, dispersity, 5% degradation temperatures (under N$_2$), and T$_g$ values for **9a-b.**

Polymer	Ratio of x:(1-x)	%Yield	M$_n$ (Da)	Đ	T$_{d-5\%}$ (^{0}C)	T$_g$ (^{0}C)
9a	0.10:0.90	95.0	8,800	2.0	-	-
9b	0.25:0.75	87.7	20,400	2.4	389	193

Molecular weight and thermal analysis characterization results for **9a-b** are summarized in **Table 1**. The percent yields, 95% and 88%, were quite good. The molecular weights and dispersity values of the copolymers were determined using size exclusion chromatography (SEC). The mobile phase used was 5% (v/v) acetic acid THF solution. The SEC traces for **9a-b** are overlaid in **Figure 29.**

The determined M$_n$ values for polymers **9b** was 20,400 Da with a relatively low dispersity of 2.4, and the M$_n$ values for **9a** was 8,800 Da with an even lower dispersity of 2.0. These M$_n$ values are relatively low but exceed the critical chain entanglement length

(3,500 Da) necessary for chain entanglements and the formation of viable film formation.[32] The lower molecular weight for **9a** could be due to incomplete conversion of the fluorine groups or formation of cyclic species during the polymerization process.
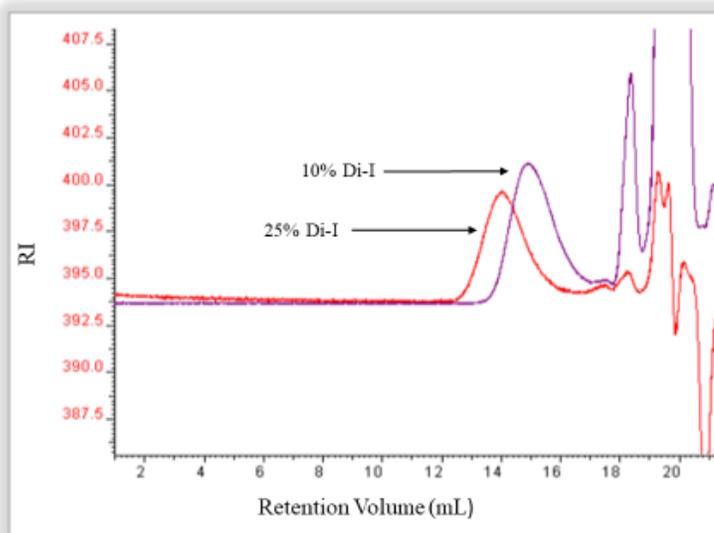
Figure 29. SEC traces for **9a-b.**

The 25% DI-Copolymer, **9b**, showed a M_n of 20,400 Da. The copolymer displayed a 5% weight loss temperature, $T_{d-5\%}$, of 389 ^{0}C and glass transition temperature, T_g, of 193 ^{0}C. For comparison purposes, Picker observed a $T_{d-5\%}$, of 413 ^{0}C for a 25 % copolymer of 3,5-difluoro-1-((3-iodophenyl)sulfonyl)benzene, with DPS and BPA (**Scheme 4**), and a T_g value of 172 ^{0}C. When the 25 % copolymer of a monomer where the iodo group was replaced with a carbazole moiety, the polymer showed the $T_{d-5\%}$ at 437 ^{0}C, under a nitrogen atmosphere and Tg = 181 ^{0}C. Thus, even though logistics prohibited the acquisition of thermal stability data for the copolymers that were subsequently prepared with carbazole, phenoxazine, and indole donors (**10a-b**, **12a-b**, and **13a-b**), it is anticipated that their thermal properties should be sufficient for OLED applications.

3.6 "Post" Functionalization of copolymers (9a-b) with (CBZ)

"Post" functionalization required the synthesis of the base polymers, **9a-b**, using monomer **3** and the comonomers bisphenol-A and DFDPS to achieve different level of functionalization, as shown in **Scheme 14**. The desired electron rich donor groups were then installed on the base polymers, after polymerization had occurred. "Post" functionalization was done by introducing different electron-rich *N*-heterocycles, like carbazole, phenoxazine, and indole. For the initial, proof of concept systems, the standard PAES monomer **3**, DFDPS **1**, was used to prepare the base polymers, however, future work might include the use of polymer backbone consisting a potential OLED host material instead. The best modification results were obtained using the following reaction protocol: copolymer **9a-b** and different electron-rich *N*-heterocycles (CBZ, PXZ, and IND), were reacted in the presence of CuI catalyst, using L-proline as the ligand, in the solvent mixture DMSO/NMP (2:1) with K_2CO_3 used as the base at 90 ^{0}C.
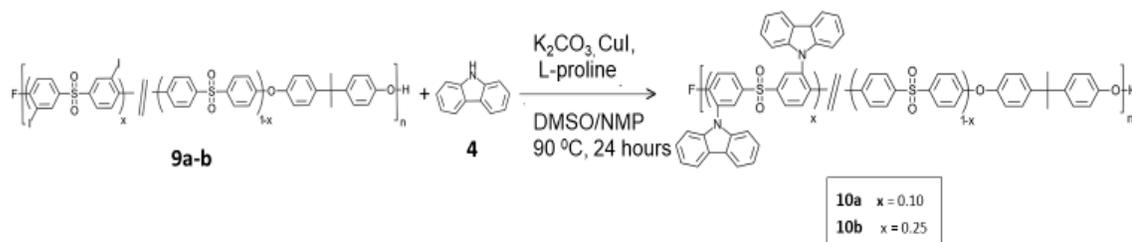
Scheme 14. Synthesis of CBZ + BPA/DPS copolymer.

Initial post-functionalization was done by introducing the electron -rich *N*-heterocycle, carbazole (**4**), to copolymers **9a-b** using a copper-catalyzed carbon-nitrogen (C-N) coupling reaction. An excess of carbazole was used in the reaction, L-proline was used as a ligand with CuI catalyst (see **Scheme 14**), DMSO and NMP in 2:1 ratio were used as solvents with K_2CO_3 used as the base and the reaction was run at 90 ^{0}C .

After 24 hours the reaction mixture was added dropwise to vigorously stirred DI

water and the resulting solid was isolated via vacuum filtration. The product was left to
dry using the vacuum for overnight. The precipitate was triturated, with approximately
200 mL ethanol, for about 2 hours and the solids were isolated via vacuum filtration,
followed by drying overnight. The solids were then dried to constant mass in a drying
pistol to afford 0.09 g (~58%) of the desired carbazole containing PAES. Introduction of
the carbazole moieties to afford the zig-zag oriented chromophore containing polymers
was confirmed via ^{1}H NMR and ^{13}C (CDCl$_3$) NMR spectra, given in **Figure 30** and
Figure 31, respectively.
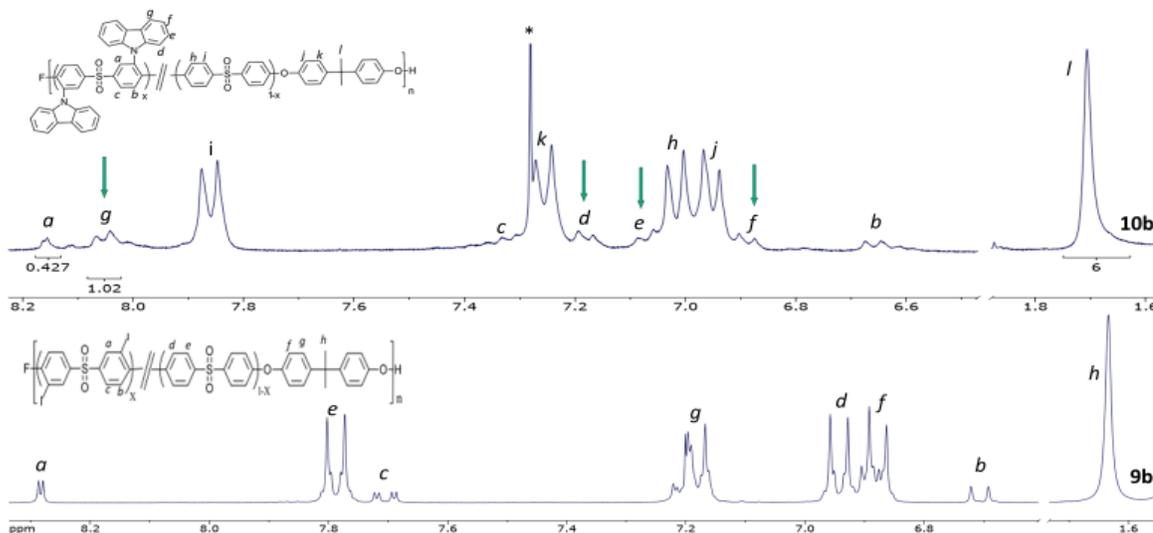
Figure 30. 300 MHz ^{1}H (CDCl$_3$) NMR spectral overlay of **9b** (25% DI) and **10b** (*
indicates CHCl$_3$).

The 300 MHz ^{1}H (CDCl$_3$) NMR spectra of **10a,b** show 11 unique signals and supports
the successful incorporation of **4** (carbazole), via substitution of the iodo groups, into the
polymer containing monomer **3**, BPA and DPS. With the substitution of the carbazole
group, the signals ***a***, ***b***, and ***c*** have been shifted more upfield, protons ***a*** at ~8.05 ppm, ***b*** at
6.65 ppm, and ***c*** at 7.17 ppm, shifted from what was observed in **9a-b**. The protons (8H)
of carbazole group can be observed with ***d*** appearing as a doublet at 8.16 ppm, ***e***

48

appearing as a doublet on 7.05 ppm, *f* appearing as a doublet at 6.85 ppm, and *g* as a doublet at 8.16 ppm.

The ratio of **3,** now substituted with two carbazole units, to **8** can be confirmed via comparison of the integration of proton signal *l* to *a* plus *g*. Calibrating the *l* signal to 6 protons (isopropyl methyl groups), results in a calculated *a* plus *g* integration of 1.45**:**6 for **10b**. Because *a* and *g* combined account for 6 protons of **3**, 1.45 can be divided by 6 and results in 0.241, which is representative of the ratio of **3** compared to **8**. The desired amount of **3** in **10b** was 25% and integration indicates that ~ 24.1% incorporation was achieved. An integration ratio 0.61**:**6 is observed for **10a**, indicating that ~10% incorporation was achieved.

Alternatively, the replacement of two iodo groups by CBZ moiety can be proved by the integration of the all protons relative to *l* (isopropyl methyl groups). As 100% of **8** (BPA) was used, it will contribute (8+6) 14 protons, 75% of **1** (DPS) was used, it will contribute (8×0.75) 6 protons, and 25% of **3** was used, and it will contribute (6+8+8=22)×0.25) = 5.5) protons. So, the total number of protons, including two CBZ units was calculated as 25.5. Based off the integrations of all aromatic protons relative to *l* (isopropyl methyl groups), results in a calculated integration value of 27.1, which is close to the desired amount of 25.5, which confirms the successful incorporation of two carbazole (**4**) units into each substituted DPS unit in the polymer backbone.

The 75.5 MHz ^{13}C (CDCl$_3$) NMR spectrum (**Figure 31**) further support the

49
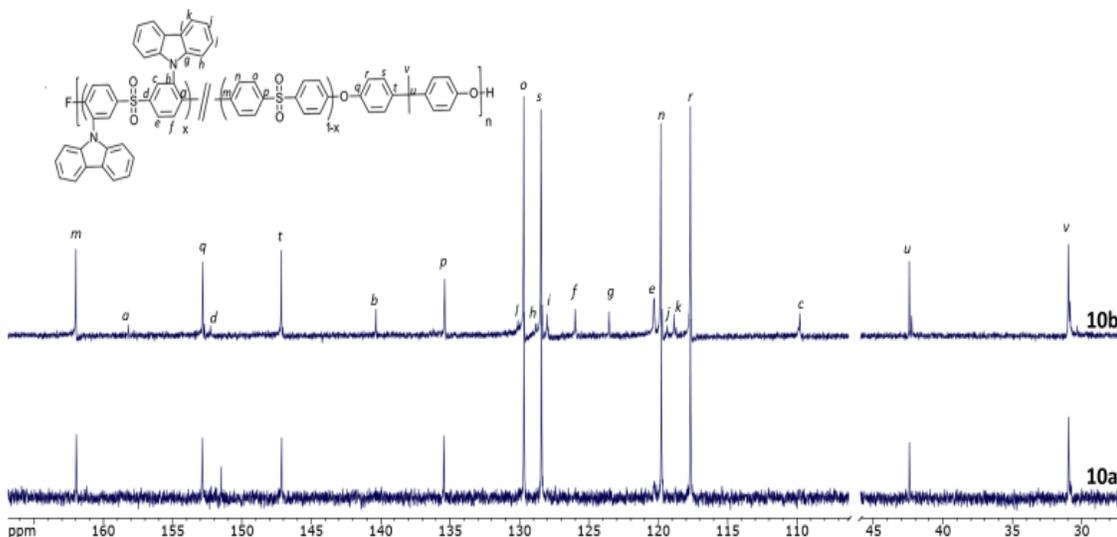
Figure 31. Overlay of 75.5 MHz ^{13}C (CDCl$_3$) NMR of **10a-b.**

incorporation of **4** into the polymer backbone system. The spectrum shows 22 unique carbon atom signals, with 6 new signals introduced from the substitution of the carbazole group. These new carbons were labelled as *g*, *h*, *i*, *j*, *k*, and *l*. The carbon signal, **b**, at ~ 140 ppm shows the formation of C-N bond. Carbon signals corresponding to **3** can be observed to slightly increase in intensity from **10a** to **10b**, and carbon signals corresponding to the DPS comonomer can be observed to slightly decrease from **10a** to **10b**.

Size exclusion chromatography (SEC) was used to determine the molecular weight and dispersity of the copolymers. The mobile phase used was 5% (v/v) acetic acid THF solution. The SEC trace of **10b** are overlaid in the **Figure 32**. The M$_n$ value for **10b** copolymer is very similar to M$_n$ of **9b** values.
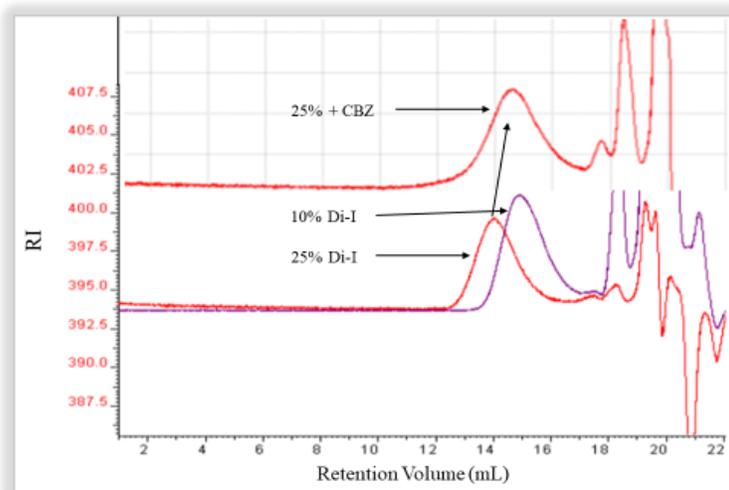
Figure 32. SEC traces of **10b.d**

3.7 "Post" Functionalization of copolymers (9a-b) with PXZ,11
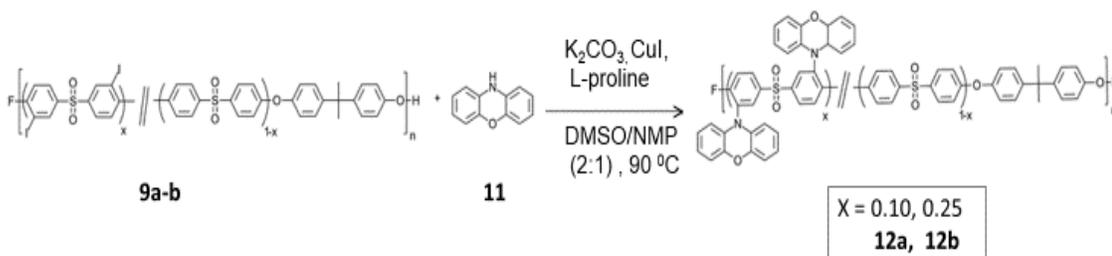
Scheme 15. Synthesis of PXZ + BPA/DPS copolymer

Post functionalization of copolymers **9a-b,** was also done by introducing an electron-rich *N*-heterocycle, phenoxazine (**11**) into copolymers **9a-b** using a copper-catalyzed carbon-nitrogen (C-N) coupling reaction. An excess of phenoxazine was used in the reaction, L-proline was used as a ligand with CuI catalyst, DMSO and NMP in 2:1 ratio were used as solvents with K_2CO_3 used as the base and the reaction was run at 90 ^{0}C.

After 24 hours, the reaction mixture was added, dropwise to the vigorously stirred

51

DI water and resulting solid was isolated via vacuum filtration. The product was left to dry over the vacuum for overnight. The precipitate was stirred with approximately 200 mL ethanol for about 2 hours. The solids were isolated via vacuum filtration and the product was left to dry overnight to afford 0.167 g (~ 91.6 %) of the desired polymer. Introduction of the phenoxazine moieties to afford the chromophore functionalized polymers was confirmed via ^{1}H NMR and ^{13}C (CDCl$_3$) NMR spectra, given in **Figure 33** and **Figure 34**, respectively.
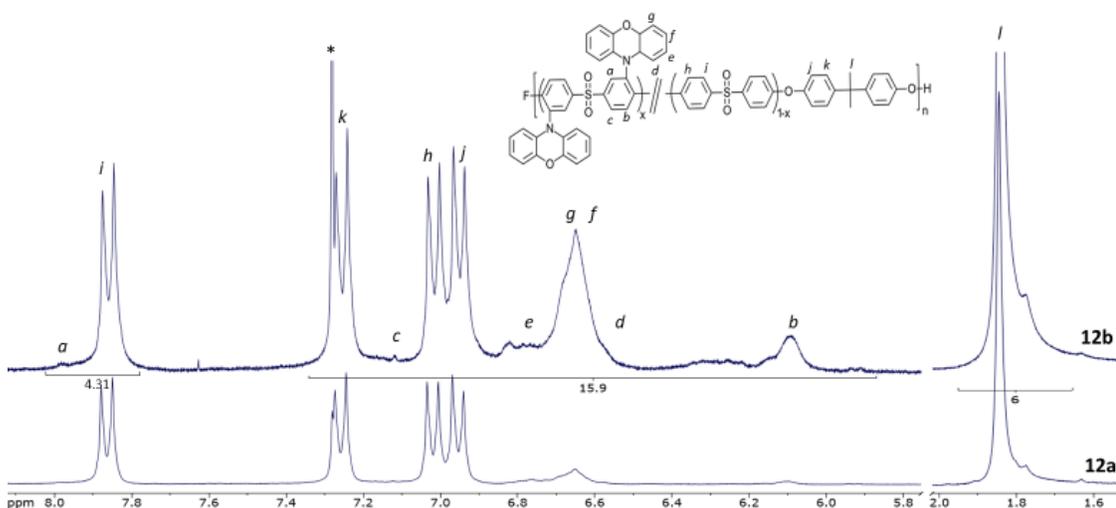
Figure 33. 300 MHz ^{1}H (CDCl$_3$) NMR of **12a-b.**

The 300 MHz ^{1}H (CDCl$_3$) NMR spectra of **12a-b** show the incorporation of **11** into the polymer containing DI-monomer **3**, DPS and bisphenol-A. The increasing concentration of **3** and **11** can be observed by an increase in the intensity of the signals assigned to protons *a*, *b*, *e*, *g*, *f*, *c*, and *d* when comparing **12a** and **12b**. The incorporation of **11** in the copolymer can be observed in protons *d*, *e*, *f*, and *g*. The integration of the all aromatic protons relative to *l* (isopropyl methyl groups), was used to confirm the incorporation of two phenoxazine (**11**) units into each functionalized DPS unit of the polymer backbone. When observing **12b**, the total number of hydrogens was 26.21, which was close to the calculated value 25.5, indicate that the two PXZ units were

52

incorporated into each unit that previously had two iodo groups.

The 75.5 MHz ^{13}C (CDCl$_3$) NMR spectra (**Figure 34**) show 22 unique carbon atom signals, with 6 new signals introduced from the substitution of the phenoxazine group. These new carbons were labelled as **g**, **h**, **i**, **j**, **k**, and **l**. As the concentration of monomer **3** increased, the intensities of the peaks increased accordingly.
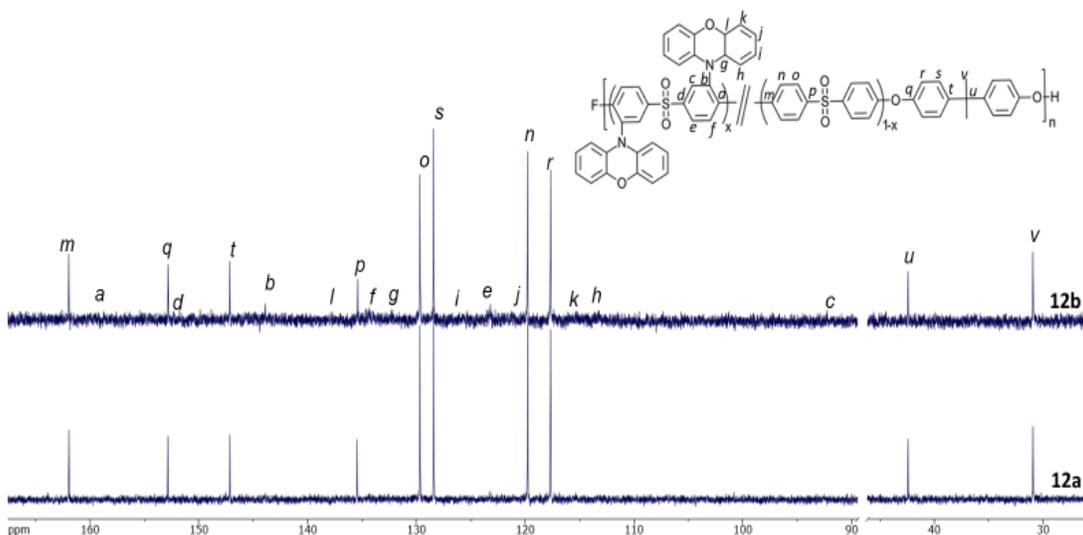
Figure 34. Overlay of 75.5 MHz ^{13}C (CDCl$_3$) NMR of **12a-b.**

3.8 "Post" Functionalization of (9a-b) with Indole, 5
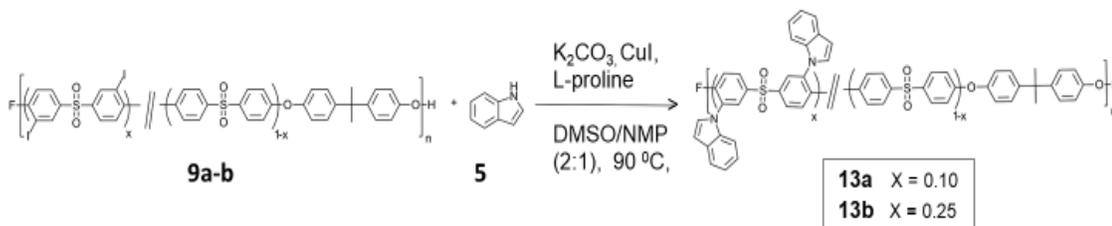
Scheme 16. Synthesis of Indole + BPA/DPS copolymer.

53

Finally, post functionalization of copolymers **9a-b**, was done by introducing an electron-rich *N*-heterocycle, indole (**5**) into copolymers **9a-b** using a copper-catalyzed carbon-nitrogen (C-N) coupling reaction. An excess of Indole was used in the reaction, L-proline was used as a ligand with CuI catalyst, DMSO and NMP in 2:1 ratio were used as solvents with K_2CO_3 used as the base and the reaction was run at 90 ^{0}C .

After 24 hours the reaction mixture was added dropwise to vigorously stirred DI water and the resulting solid was isolated via vacuum filtration and left to dry over the vacuum for overnight. The precipitate was stirred with approximately 200 mL ethanol for about 2 hours and the solids were isolated via vacuum filtration and the product was left to dry overnight to afford 0.148 g (~ 74.5%) of the desired polymer. Introduction of the indole moieties to afford the chromophore functionalized polymers was confirmed via their ^{1}H NMR and ^{13}C (CDCl$_3$) NMR spectra, as given in **Figure 35** and **Figure 36**, respectively.
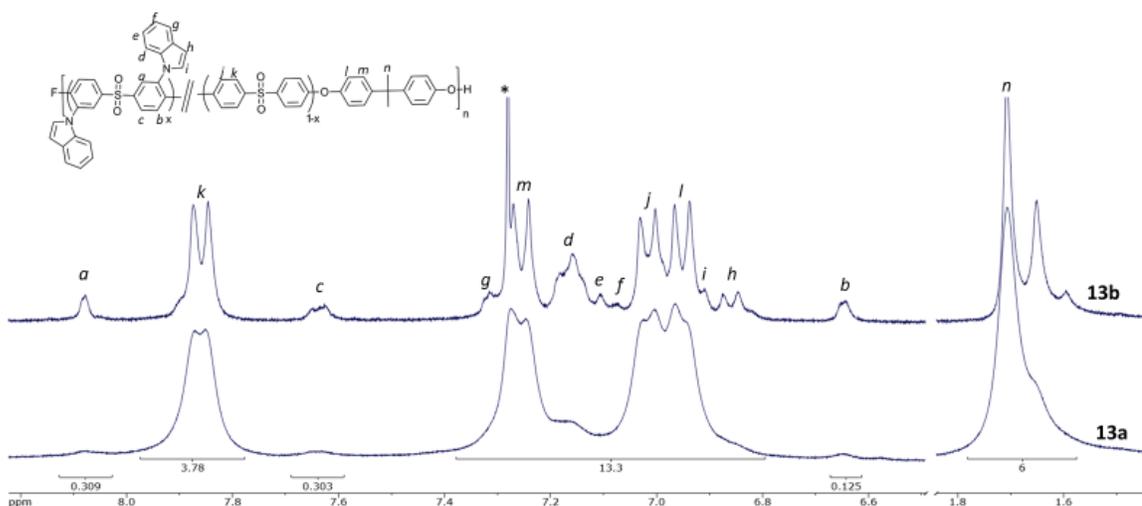
Figure 35. 300 MHz ^{1}H (CDCl$_3$) NMR of **13a-b.**

The 300 MHz ^{1}H (CDCl$_3$) NMR spectra of **13a-b** confirm the incorporation of

5 into the polymer containing DI-monomer **3**, DPS and Bisphenol-A. The increasing concentration of **3** and **5** can be observed by an increase in the intensity of the signals assigned to protons *a*, *c*, *g*, *d*, *e*, *f*, *i*, *h* and *b* when comparing **13a** and **13b**. The incorporation of **5** in the copolymer can be observed in protons *d*, *e*, *f*, *g*, *h* and *i*. The integration of the all aromatic protons relative to *n* demonstrate the incorporation of two indole (**5**) units into each of the functionalized DPS units of the polymer backbone. When observing **13a**, the total number hydrogens are 23.82 (all aromatic and aliphatic), relative to the methyl groups in the isopropyl groups are close to the calculated value 23.0, indicate that the two IND units were incorporated into each unit that previously had two iodo groups.

The 75.5 MHz ^{13}C (CDCl$_3$) NMR spectra (**Figure 36**) show 24unique carbon atom signals, with 8 new signals introduced from the indole groups. These new carbons were labelled as *g*, *h*, *i*, *j*, *k*, *l*, *m*, and *n*.
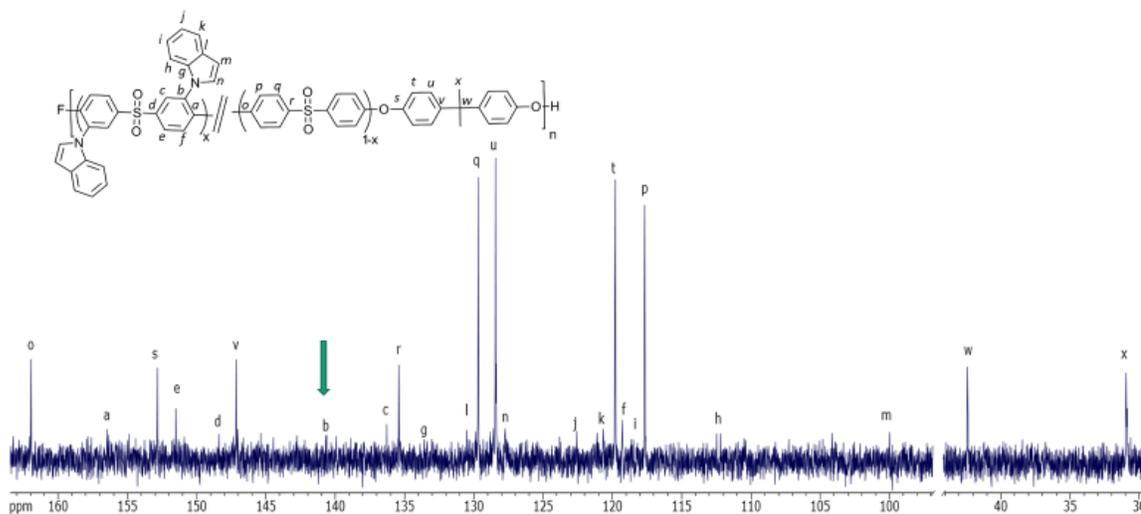
Figure 36. 75.5 MHz ^{13}C (CDCl$_3$) NMR of **13b.**

3.9 Optical Properties of Copolymers

The optical properties of the chromophore containing PAE systems were

55

studied by a combination of UV/Vis and fluorescence spectroscopy. Ultraviolet-visible spectroscopy (UV/Vis) refers to absorption spectroscopy. This means it uses light in the visible and adjacent ranges. Absorption spectroscopy is complementary to fluorescence spectroscopy, in that fluorescence deals with transitions from the excited state to the ground state, while absorption measures transitions from the ground state to the excited state. UV/Vis spectra were acquired in order to determine the appropriate wavelengths for fluorescent spectroscopy. These wavelengths were utilized to excite the polymer to acquire fluorescent data of the different copolymers.

Spectroscopic analysis is commonly carried out in solutions and, in the present case, polymer absorption and fluorescence data were acquired in THF, or 5% (v/v) acetic acid THF solutions at a concentration of 20 µM. Solutions of each copolymers were prepared to similar concentrations of approximately 20 µM to minimize the variation of results due to concentration differences. All copolymer solutions showed both strong and weak absorptions in the absorbance spectra (**Figure 37a**, **Figure 38a**, and **Figure 39a**).

Photophysical analysis of copolymer **9b,** the base polymer, without any chromophore in it and chromophore polymer **10b** were performed via UV/Vis and fluorescence spectroscopy. The copolymers **9b** and **10b** displayed a major absorption peak at 265 nm due to phenyl groups. Chromophore containing polymer **10b**, showed absorption wavelengths of 265 nm and 340 nm, with later absorption due to the donor-π-acceptor system while copolymer **9b** showed no absorbance in this region. The solution fluorescence data of 25% DI-copolymer, **9b** and copolymer containing 25% chromophore, **10b**, in THF are shown in **Figure 37.**

Fluorescence spectroscopy was performed using 300 nm and 340 nm as the excitation wavelengths. Copolymer **9b** displayed low intensity emission around 362 nm when excited at 300 nm. The carbazole based copolymer **10b**, displayed an emission wavelength of about ~ 416 nm when excited at 340 nm.
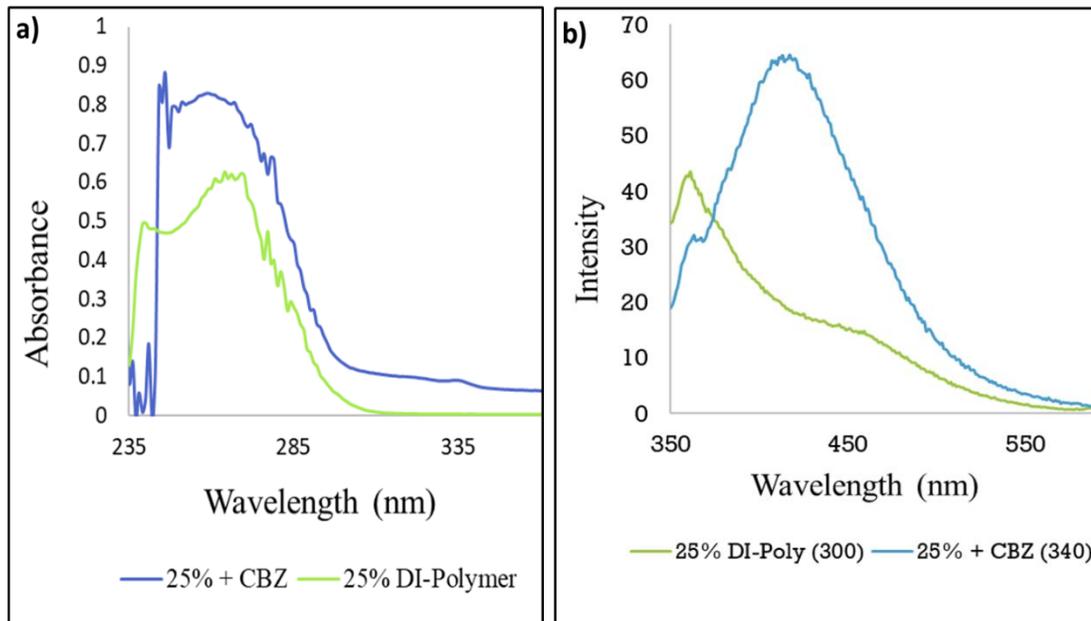
Figure 37. Absorption (a) and emission (b) spectra of 25% DI-Copolymer, **9a** and 25% carbazole copolymer, **10b** solutions in THF and 5% Acetic Acid THF solution, respectively, at 20 µM.

The modified copolymer with carbazole (**10a-b**) showed poor solubility in THF, and so, a 5% (v/v) acetic acid THF solution was used to make 20 µM copolymer solutions for analysis.

Figure 38 illustrates the UV/Vis and fluorescence spectra of polymers **10a-b** acquired in 5% (v/v) acetic acid THF solution. The strongest absorption for copolymers **10a-b** occurred at 265 nm due to the phenyl groups within the compound and a distinct shoulder centered at 340 nm indicating the absorption due to the chromophore unit. Copolymer **10b** showed two-fold more intensity than that of **10a**, at ~ 416 nm, when excited at 340 nm. Copolymer **10b,** containing 25% chromophore showed the highest fluorescence intensity due to its higher percentage of CBZ chromophore in the polymer, while 10% copolymer **10a**, showed the weak fluorescence at ~ 412 nm due to a lower percentage of the chromophore.
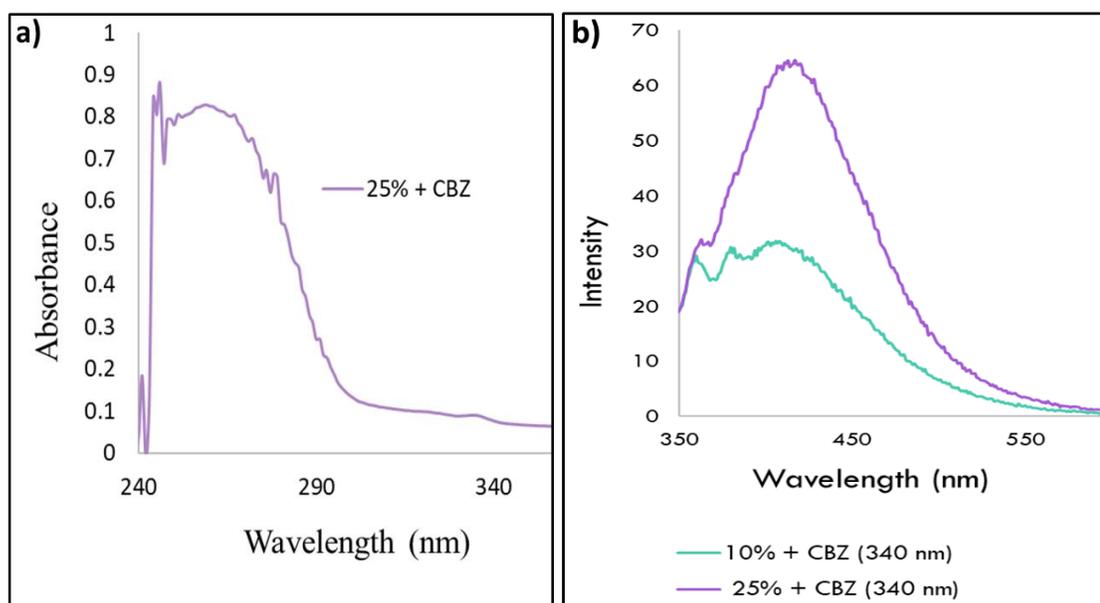
Figure 38. Absorption (a) and emission (b) spectra of copolymers (**10a-b**) solutions in 5% acetic acid THF solution, at a concentrations of 20 µM.

The phenoxazine based copolymers **12a-b** showed strong and weak absorptions in their UV/Vis absorption spectra (**Figure 39a**). The strongest absorption occurred at 265 nm, due to phenyl groups within the copolymer. The distinct shoulders at wavelengths of 325 nm and 340 nm indicate the absorptions due to the chromophore units.

Copolymers **12a-b** were excited at 325 nm, and 340 nm. An overlay of fluorescence spectra of **12a-b,** excited at 325 nm and 340 nm, is shown in **Figure 39b.**

Emission behaviors varied depending on the excitation wavelength. The 10% and 25% PXZ based copolymers showed maximum fluorescence peaks, ranging from 403 nm to 410 nm, when excited at 325 nm and 340 nm (**Figure 39b**). Polymer **12b,** showed the highest fluorescence intensity due to the higher percentage of chromophore in the polymer. It can be clearly interpreted that, at the excitation wavelength of 325 nm, the emission spectrum for **12b** showed intensity almost two-fold that of **12a**. Copolymer **12b**
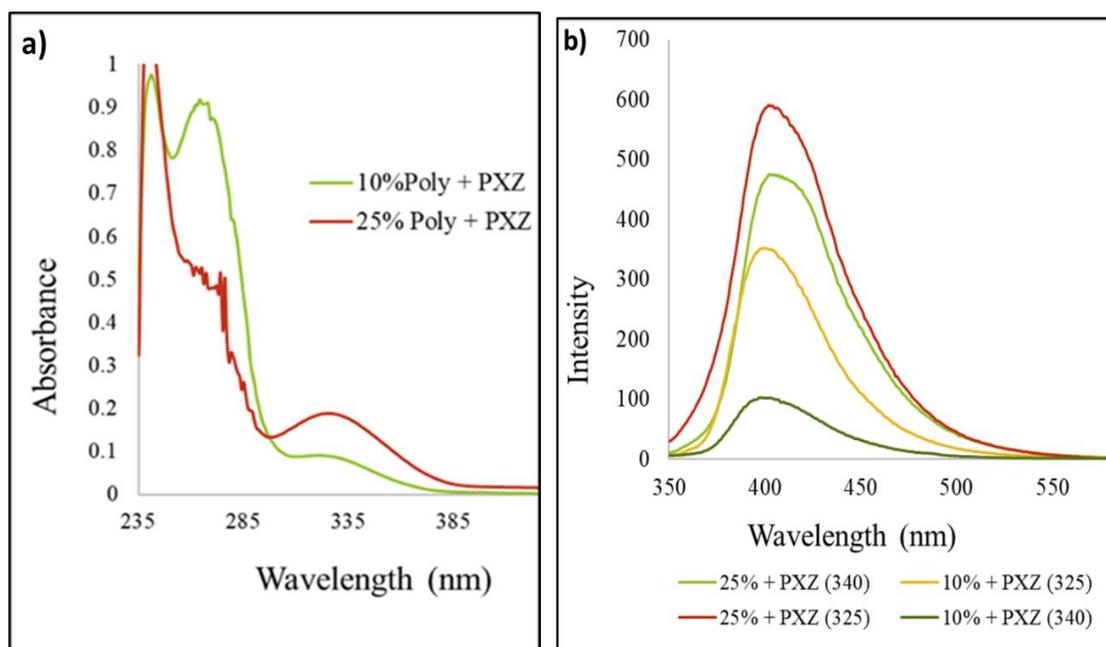
Figure 39. Absorption (a) and emission (b) spectra of copolymers (**12a-b**) solutions in THF, at 20 µM.

showed peak emission at ~ 410 nm, while copolymer **12a** showed a peak intensity at ~ 403 nm, when excited at 325 nm. An excitation wavelength of 325 nm gave much stronger emission than the excitation using 340 nm, with **12b** showing approximately 30 % stronger emission.

The indole based copolymers, **13a-b,** showed strong and weak absorptions in their UV/Vis absorption spectra (**Figure 40a**). The absorption spectra of copolymers **13a-b** were acquired in THF at a concentration of 20 µM. Copolymers **13a-b** were excited at 265 nm and 305 nm as displayed in **Figure 40**. The copolymer, **13a-b,** showed strongest absorption at ~ 265 nm and ~ 305 nm. Copolymers **13a-b** showed the highest emission intensity at ~ 435 nm, when excited at 305 nm, while copolymer **13b** showed three-fold more intense signal than **13a**. Although the emission corresponding to the excitation at 265 nm appears at ~ 455 nm, it is noticeably less intense than the emission, when excited at 305 nm.
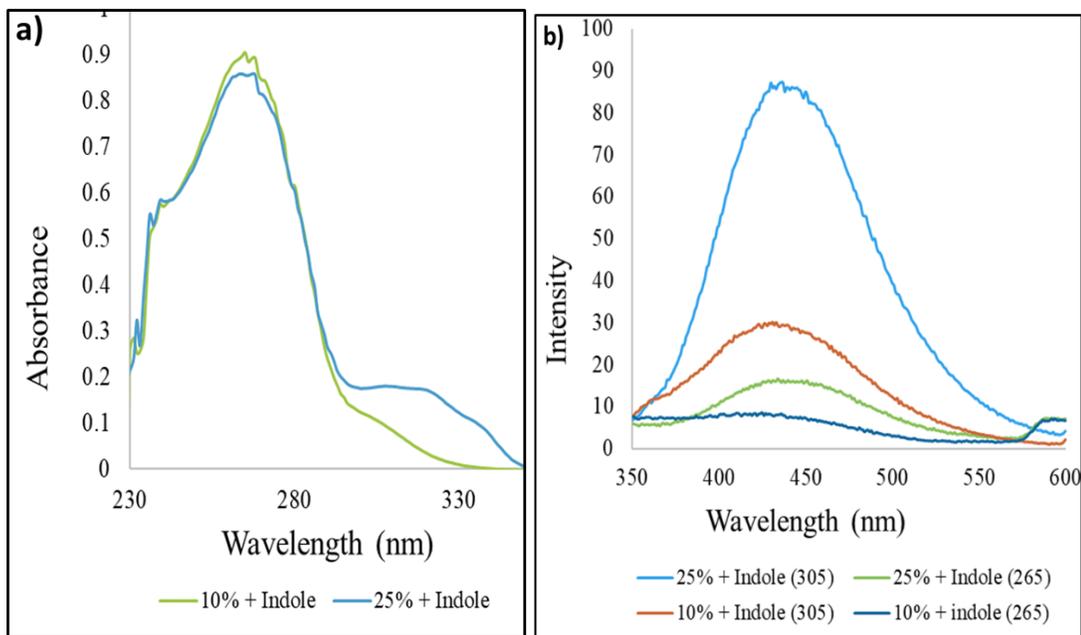
Figure 40. Absorption (a) and emission (b) spectra of copolymers (**13a-b**) solutions in THF, 20 µM.

An overlay of the fluorescence spectra of copolymers **9b**, **10b**, **12b**, and **13b** is shown in **Figure 41**. The fluorescence data of all the copolymers, was acquired in THF and a 5% (v/v) acetic acid THF solutions at a concentration of 20 µM. Solutions of each of the copolymers were prepared to similar concentrations of approximately 20 µM to minimize variation of results due to concentration differences. Copolymer **12b** showed the most intense signals, almost five-fold more intense than the **10b** and **13b** while copolymer **10b** and **12b** showed similar intense signals. The copolymer **10b** showed an emission peak at ~ 414 nm, and the copolymer **12b** gave at 410 nm.
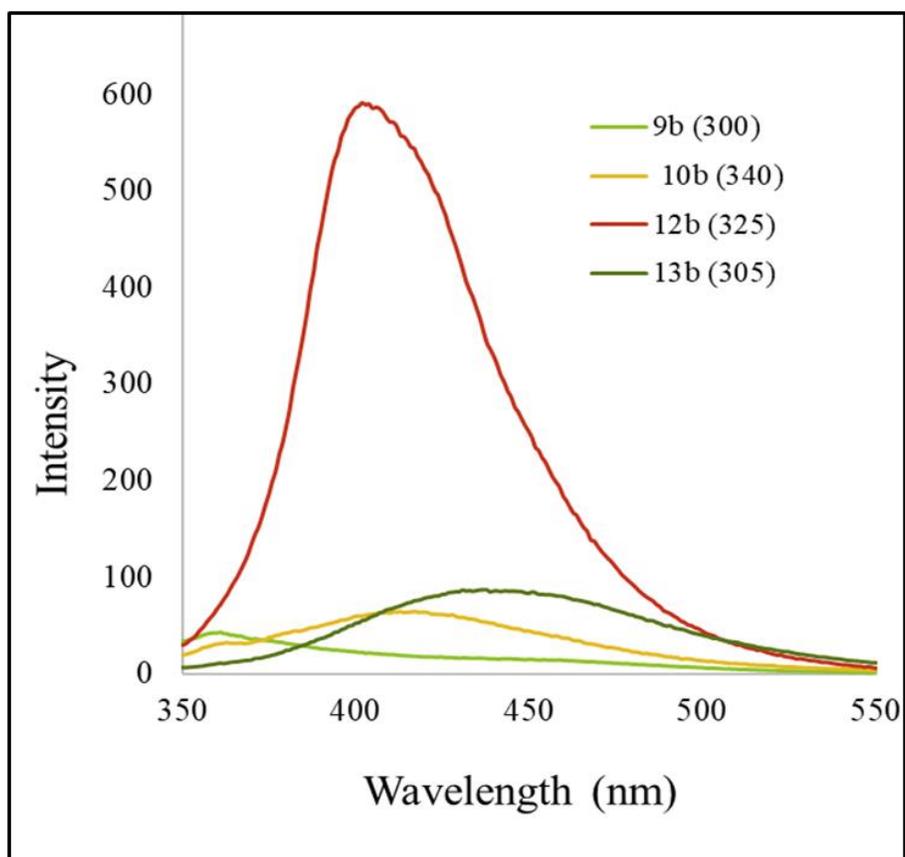
Figure 41. An overlay fluorescence spectra of copolymers **9b** (Di-iodo), **10b** (CBZ), **12b** (PXZ), and **13b** (IND) solutions in THF, 20 µM. Excitation wavelengths used were 300nm, 340 nm, 325 nm, and 305 nm.

4. CONCLUSION

The syntheses of a (DI-DFDPS) monomer, **3** and the subsequent preparation of a copolymer series were successfully achieved with excellent yield and purity. The structure of the monomeric species was confirmed by GC/MS analysis, NMR spectroscopy, and elemental analysis. The "pre" functionalization route was investigated to synthesize a sulfone/carbazole-functionalized monomer for incorporation into a **PAES** copolymers but this "pre" functionalization technique was unsuccessful. The Di-iodo monomer (**3**) was successfully incorporated into the polymeric backbones by using 4,4'-difluorodiphenylsulfone (DFDPS), **1**, and bisphenol-A (BPA), **8**, via NAS polycondensation reactions. The structures of the polymers were confirmed by NMR spectroscopy and their properties were characterized by TGA, DSC, and SEC analyses.

The 10% DI-Copolymer, **9a**, and 25% DI-Copolymer, **9b**, were subjected to copper-catalyzed carbon-nitrogen bond forming reactions using the *N*-heterocycles: carbazole, phenoxazine and indole. Copolymers **9a-b** were modified via a "post" polymerization process using different *N*-heterocycles like carbazole, phenoxazine and indole. A total of eight copolymers were prepared in this project, out of eight, two, **9a-b**, were prepared by varying the percentages of **1** and **3**, and the remainder were prepared by introducing carbazole, phenoxazine and indole to **9a-b**.

The optical properties of the copolymers in solution were evaluated by a combination of UV/Vis and fluorescence spectroscopy. All of the copolymers displayed both weak and strong absorptions in the ultra-violet spectra with the strongest absorptions due to the phenyl groups, centered at about 270 nm, along with longer wavelength

absorptions due to the chromophore units. The chromophores all exhibited common absorptions ranging from 305 nm to 340 nm. When excited at 340 nm, copolymer **10a-b** (CBZ), exhibited peak wavelength of emission at ~ 410 nm in a 5% (v/v) acetic acid THF solutions at a concentration of 20 µM. When excited at 325 nm, copolymers **12a-b** (PXZ), exhibited maximum wavelength emission at ~ 403 and ~ 410 nm, respectively. When excited at 265 nm, the copolymer **13a-b** (IND), showed emission peaks centered at ~ 419 nm and ~ 436 nm, respectively. When excited at 305 nm, the copolymer **13a-b**, showed emission peaks centered at ~ 430 nm and ~ 438 nm, respectively.

5. PROPOSED FUTURE WORK

Current studies have shown the potential for development of blue OLED emitters based on carbazole, phenoxazine and indole, via a post polymerization methodology. The di-iodo monomer can be easily polymerized to form PAE-based fluorescent polymers for OLED applications.

The methods developed in this thesis can serve as a starting point for the synthesis of a wide variety of new monomers and polymers. The "pre" functionalization for monomer, **3** was unsuccessful, however with alternative catalysts, ligands, and different reaction conditions may allow that pathway to proceed. The use of a "post" functionalized route should be further investigated to introduce other donor groups like, phenothiazine and acridine. Other colors could be obtained using various donor groups with **3**. Finally, the use of other catalysts, such as Pd and Ni, should be investigated to determine if the limitations of copper catalysts may be overcome.

6. REFERENCES

1.   Tang, C. W.; VanSlyke, S. A. Organic electroluminescent diodes. *Appl. Phys. Lett*. **1987**, *51*, 913.

2.   "Sony Corporation Global Headquarters." Sony Global. N.p., n.d. Web. **24 July 2014.**

3.   Pereira, Luiz. "Organic Light-emitting Diodes: The Use of Rare-earth and Transition Metals." Singapore: Pan Stanford Pub., **2012.** Print.

4.   Yousefi, M. H.; Fallahzada, A.; Saghaei, J.; Darareh, M. D., Fabrication of Flexible ITO-Free OLED Using Vapor-Treated PEDOT:PSS Thin Film as Anode. *Journal of Display Technology,* **2016,**12, 1647-1651

5.   Gupta, A.; Watkins, S. E.; Scully, A. D.; Singh, T. B.; Wilson, G. J.; Evans, R. A., Band- gap tuning of pendant polymers for organic light-emitting devices and photovoltaic applications. *Synth. Met*. **2011**, 161, 856-863.

6.   Kafafi, Z. H., *Organic electroluminescence*. CRC Press, Taylor & Francis: Boca Raton, FL, 2005.

7.   Volz, D.; Review of organic light-emitting diodes with thermally activated delayed fluorescence emitters for energy-efficient sustainable light sources and displays. *J. Photonics Energy* **2016**, 6 (2), 020901.

8.   Minaev, B.; Baryshnikov, G.; Agren, H., Principles of Phosphorescent Organic Light-Emitting Devices. Phys. Chem. Chem. Phys. 2014, 16, 1719-1758.

9.   Kim, S. O.; Lee, K. H.; Kim, G. Y.; Seo, J. H.; Yoon, S. S., A Highly Efficient

Deep Blue fluorescent OLED based on diphenylaminofluorenylstyrene-containing emitting materials. *Synth. Met.* **2010**, 160, 1259-1265.

10.   Fu, H.; Zhan, Y.; Xu, J.; Hou, X.; Xiao, F., Red Fluorescent materials based on naphthylamine for non-doping OLEDs. *Optical Materials* **2006**, 29 (2), 348-354.

11.   Zhang, Q. S.; Li, J.; Shizu, K.; Huang, S. P.; Hirata, S.; Miyazaki, H.; Adachi, C., Design of Efficient Thermally Activated Delayed Fluorescence Materials for Pure Blue Organic Light Emitting Diodes. *J. Am. Chem. Soc.* **2012**, 134, 14706-14709.

12.   Yu, M. X.; Duan , J. P.; Lin, C. H.; Cheng, C. H.; Tao, Y. T., Diaminoanthracene

Derivatives as High-Performance Green Host Electroluminescent Materials. *Chemistry of Materials* **2002**, *14* (9), 3958.

13.   Rajamalli, P.; Chen, D.; Li, W.; Samuel, I. D. W.; Cordes, D. B.; Slawin, A. M. Z.; Zysman-Colman, E., Enhanced Thermally Activated Delayed Fluorescence through Bridge Modification in Sulfone-Based Emitters Employed in Deep Blue Organic Light-Emitting Diodes. *Journal of Materials Chemistry* **2019**, *7* (22), 6664–6671.

14.   Nobuyaus, R. S.; Ren, Z.; Griffins, G. C.; Batsanov, A. S.; Data, P.; Yan, S.; Monkman, A. P.; Bryce, M. R.; Dias, F. B.; Rational design of TADF Polymers Using a Donor-Acceptor Monomer with Enhanced TADF Efficiency Induced by the Energy Alignment of Charge Transfer and Local Triplet Excited States. *Adv. Optical Materials* **2016**, 4 (4), 597.

15.   Xie, Y.; Li, Z.; Thermally Activated Delayed Fluorescent Polymers. *Journal of Polymer Science, Part A: Polymer Chemistry* **2017**, 55, 575-584.

16.   Yun, J. H.; Lee, J. Y., Benzoisoquinoline-1,3-dione Acceptor Based Red

Thermally Activated Delayed Fluorescent Emitters. *Dyes and Pigments* **2017**, 144 (2017) 212-217

17.   Stachelek, P.; War, Jonathan S.; Santos, Paloma L. dos.; Danos, A.; Colella, M.; Haase, N.; Raynes, Samuel .J.; Batsanov, Andrei S.; Bryce, Martin R.; Monkman, A. P., Molecular Design Strategies for Color Tuning of Blue TADF Emitters. *ACS Applied Materials & Interfaces* **2019**, 11 (30) 27125-27133.

18.   Huang, B.; Ban, X.; Sun, K.; Ma, Z; Mei, Y.; Jiang, W.; Lin, B.; Sun, Y., Thermally activated delayed fluorescence materials based on benzophenone derivatives as emitter for efficient solution-processed non-doped green OLED. *Dyes and Pigments* **2016**, 133, 380-386.

19.   Li, Jie.; Zhang, R.; Wang, Z.; Zhao, B.; Xie, J.; Zhang, F.; Wang, H.; and Guo, K., Zig-Zag Acridine/Sulfone Derivative with Aggregation-Induced Emission and Enhanced Thermally Activated Delayed Fluorescence in Amorphous Phase for Highly Efficient Nondoped Blue Organic Light-Emitting Diodes. *Adv. Optical Mater*. **2018**, *6*, 1701256.

20.   Liu, Y.; Wang, Y.; Li, C.; Ren, Z.; Ma, D.; Yan, S., Efficient Thermally Activated Delayed Fluorescence Conjugated Polymeric Emitters with Tunable Nature of Excited States Regulated via Carbazole Derivatives for Solution-Processed OLEDs. *Macromolecules* **2018**, *51* (12), 4615-4623.

21.   Li, Z.; Ren, Z.; Sun, X.; Li, H.; Yan, S., Deep-Blue Thermally Activated Delayed Fluorescence Polymers for Nondoped Solution-Processed Organic Light-Emitting Diodes. *Macromolecules* **2019**, 52 (6) 2296-2303

22.   Ren, Z.; Bryce Martin, R.; Dias, Fernando, B.; Monkman, Andrew, P.; Nobuyasu

Roberto, S.; Yan, S., Pendant Homopolymer and Copolymers as Solution-Processable Thermally Activated Delayed Fluorescence Materials for Organic Light-Emitting Diodes. *Macromolecules* **2016**, *49* (15), 5452-5460.

23.   Ren, Z.; Nobuyasu, R. S.; Dias, F. B.; Monkman, A. P.; Yan, S.; Bryce, M. R. Pendant Homopolymer and Copolymers as Solution-Processable Thermally Activated Delayed Fluorescence Materials for OrganicLight-Emitting Diodes. *Macromolecules* **2016**, 49, 5452-5460.

24.   Chanda, M.; Roy, S. K., *Plastics technology handbook*. 4th ed.; CRC Press/Taylor & Francis Group: Boca Raton, FL, 2007.

25.   Bruice, P. Y., *Organic chemistry*. Seventh ed.; Pearson: New York City, NY 2014

26.   Picker, J. L.; *Routes to N-Heterocycle Functionalized Poly(arylene ether sulfone)s*. Wright State University / OhioLINK: 2014.

http://rave.ohiolink.edu.ezproxy.libraries.wright.edu/etdc/view?acc_num=wright 1409597075

27.   Tatli, M.; Selhorst, R.; Fossum, E., Poly(arylene ether)s with Pendant 3-Iodophenyl Sulfonyl Groups: Synthesis, Characterization, and Modification. *Macromolecules* **2013**, 46, 4388-4394.

28.   Meyer, L., *Structure-Property Relationships of N-Heterocycle Functionalized Triphenylphosphine Oxide-Based Poly (arylene Ether)s.* Wright State University / OhioLink: 2018.

http://rave.ohiolink.edu.ezproxy.libraries.wright.edu/etdc/view?acc_num=wright 154651093060725

29.   Kohnen, A. L.; Dunetz, J. R.; Danheiser, R. L., Synthesis of Ynamides by

N-alkynylation of Amine Derivatives. Preparation of *N*-allyl-
N-(methoxycarbonyl)-1,3-decadinylamine. *Organic Syntheses; An Annual Publication of Satisfactory Methods For The Preparation of Organic Chemicals* **2007**, 84, 88-101.

30.   Dizman, C., Tasdelen, M. A., and Yagci, Y., "Recent Advances in the Preparation of Functionalized Polysulfones", *Poly. Int*., **2013**, *62*, 991-1007

31.   Li, Nanwen.; Shin, D. W.; Hwang, D. S.; Lee, Y. M.; Guiver, M. D., Polymer Electrolyte Membranes Derived from New sulfone Monomers with Pendent Sulfonic Acid Groups. *Macromolecules* **2010**. *43*, 9810-9820

32.   Wang S, McGrath JE. In: Rogers MW, Long TE, editors. Synthetic methods in step-growth polymers. New York: John Wiley & Sons; 2003.

33.   Slaybaugh, A., *Structure-Property Relationships in PAEs Prepared From 2-(2,4-difluorophenyl)benzoxazole Derivatives.* Wright State University / OhioLINK: 2018. http://rave.ohiolink.edu.ezproxy.libraries.wright.edu/etdc/view?acc_num=wright 152653989709853

34.   Fetters, H., *Functionalized PEEK Analogues From 2,4- And 3,6-Difluorobenzophenone Derivatives.* Wright State University / OhioLINK: 2019.